A Review of Modeling, Management, and Applications of Grid-Connected Li-Ion Battery Storage Systems

Mahdi Rouholamini, *Senior Member, IEEE*, Caisheng Wang, *Senior Member, IEEE*, Hashem Nehrir, *Life Fellow, IEEE*, Xiaosong Hu, *Senior Member, IEEE*, Zechun Hu, *Senior Member, IEEE*, Hirohisa Aki, *Senior Member, IEEE*, Bo Zhao, Zhixin Miao, *Senior Member, IEEE*, and Kai Strunz, *Senior Member, IEEE*

***Abstract*—The intermittency of renewable energy sources makes the use of energy storage systems (ESSs) indispensable in modern power grids for supply-demand balancing and reliability enhancement. Besides pumped-storage hydroelectric power stations, energy storage deployment worldwide is still quite low. However, the status quo might rapidly change as the energy storage technologies are growing and facilitating market regulations are being ratified. Battery energy storage systems (BESSs), Li-ion batteries in particular, possess attractive properties and are taking over other types of storage technologies. Thus, in this article, we review and evaluate the current state of the art in managing grid-connected Li-ion BESSs and their participation in electricity markets. The review mainly includes battery modeling, the architecture of battery management systems (BMSs), the incorporation of BESSs for electricity market services, global utility-scale battery storage facilities, and challenges in implementing and managing grid-connected BESSs.**

***Index Terms*—Balancing, battery management system, degradation, grid integration, Li-ion battery, state of health.**

Manuscript received 18 June 2021; revised 13 December 2021, 11 April 2022, and 9 June 2022; accepted 18 June 2022. Date of publication 5 July 2022; date of current version 21 October 2022. The work of Mahdi Rouholamini was supported in part by the National Science Foundation of USA under Grant IIS-1724227. Paper no. TSG-00914-2021. *(Corresponding author: Caisheng Wang.)*

Mahdi Rouholamini and Caisheng Wang are with the Department of Electrical and Computer Engineering, Wayne State University, Detroit, MI 48202 USA (e-mail: gj9598@wayne.edu; cwang@wayne.edu).

Hashem Nehrir is with the Electrical Engineering Department, Montana State University, Bozeman, MT 59717 USA (e-mail: hnehrir@montana.edu).

Xiaosong Hu is with the Department of Automotive Engineering, Chongqing University, Chongqing 400044, China (e-mail: xiaosonghu@ieee.org).

Zechun Hu is with the Department of Electrical Engineering, Tsinghua University, Beijing 100084, China (e-mail: zechhu@tsinghua.edu.cn).

Hirohisa Aki is with the Faculty of Engineering, Information and Systems, University of Tsukuba, Tsukuba 305-8573, Japan (e-mail: aki@kz.tsukuba.ac.jp).

Bo Zhao is with the Center for Technology Research and Development, State Grid Zhejiang Electric Power Research Institute, Hangzhou 310014, China (e-mail: zhaobozju@163.com).

Zhixin Miao is with the Electrical Engineering Department, University of South Florida, Tampa, FL 33620 USA (e-mail: zmiao@usf.edu).

Kai Strunz is with the Department of Sustainable Electric Networks and Sources of Energy, Technische Universität Berlin, 10587 Berlin, Germany (e-mail: kai.strunz@tu-berlin.de).

Color versions of one or more figures in this article are available at https://doi.org/10.1109/TSG.2022.3188598.

Digital Object Identifier 10.1109/TSG.2022.3188598

I. Introduction

RENEWABLE energy resources, which as of now account for 22% of the total electricity supply worldwide, are widely seen indispensable when it comes to the globe's energy future, as they are abundant and avoid greenhouse gas emissions produced by conventional fossil fuel energy resources. Twenty-nine states in the U.S. have issued renewable portfolio standards that mandate 15–30% renewable electricity sales by 2025 [1]. Solar and wind power generation systems are thus moving to the forefront as the primary sources of electricity generation. Although various forecasting tools have been developed to deal with the intermittency of solar and wind energy resources, the forecasting error still remains high [2]. Therefore, energy storage is necessary to integrate these renewable energy sources into the power grid. Moreover, the need for supply-demand balancing, fast responsive frequency regulation, peak shaving and load shifting, photovoltaic (PV)/Wind smoothing, Duck curve mitigating, reliability enhancement, system restoration, energy arbitrage, and providing inertia, have also greatly prompted grid applications of energy storage [3].

There are three major storage technologies, namely, pumped-hydro, compressed air, and battery, which have been more sought after than other storage types in power systems. At present, pumped-hydro dominates the storage landscape by occupying 96% of the total installed storage capacity worldwide [4]. However, it is site-constrained and has a round-trip efficiency of about 75% if modern technology is used [5]. The compressed air, which has an efficiency of 40-52%, is geologically restricted as pumped-hydro. On the contrary, BESSs can be flexible in design and deployed almost anywhere. The battery technology and penetration are increasingly growing. The global battery stationary energy storage market is anticipated to grow exponentially, from a modest 9 GW/17 GWh deployed as of 2018 to 1,095 GW/2,850 GWh by 2040, according to the recent forecasts [6]. It is reported that the per-kWh battery cost is going to decrease to half of the 2020 price by 2030 as demand is increasing in both stationary storage and electric vehicle (EV) applications [7]. Wind and solar are anticipated to increase the current 7% share of the world's electricity supply to 40% by 2040, as wind, solar, and battery

systems costs continue to decline [6]. More importantly, the percentage of passenger EVs, which is now around 2% of the global market, could increase to 33% by 2040 [6]. This growth would add a huge scale to the battery manufacturing sector.

Due to its attractive features, i.e., high efficiency and energy density, low self-discharge rate, and rapid response (within 20 ms [8]), the BESS seems to have already emerged as a clear winner among the aforementioned storage devices [9]. The Li-ion battery has attracted the most commercial and research interest among the various kinds of battery technologies due to its higher energy density, fast charging, high reliability, portability, suitable lifespan, compact size, flexible application, and lightness. As stated by the U.S. Department of Energy (DOE), Li-ion batteries used for frequency regulation applications are among the fastest-growing energy storage markets [10]. Two-thirds of today's global battery market is dominated by Li-ion batteries [4].

Despite the above-mentioned desirable properties, Li-ion batteries have the shortcoming that they need perpetual monitoring and special control to achieve high performance and prevent early battery deterioration and potential hazards [11]–[12]. Thus, a BMS, which includes both hardware and software, is required to control the battery's operational conditions to prolong the cycle life, maintain safety, and accurately estimate the different states of the battery for energy management purposes [12].

There are some review papers in the literature that discuss battery systems. For instance, [13] presents a review over power electronics topologies for utility-scale BESS connected to medium-voltage grid. Reference [14] comprehensively reviewed commercially available battery technologies and then studied the integration of BESSs into distribution networks. The paper also reviewed power electronic converters for battery systems. Reference [15] is mainly focused on data acquisitions from battery data sheets and the estimations of battery states. In [16], the authors enumerate the different functions and corresponding control strategies of BESS in power supply, transmission and distribution sectors of power systems. There also exist other review papers in the literature that are mainly focused on particular topics such as battery state estimation and balancing [11], [17]–[20] or technologies and materials [4]. Thus, there is still a lack of analysis on the relationship between the characterization, modeling, management, and applications of grid-tied BESSs.

Many of the existing review papers investigate a specific aspect of batteries, whereas battery storage is a multidisciplinary area, which is of great interest and is being studied by different communities. For electrical power professionals who are interested in this important topic but do not have sufficient background, it is not an easy and trivial task to go through the "literature jungle" without being overwhelmed or even lost. This review paper is to address this challenge by reviewing the core background issues as well as the indispensable literature surrounding the essential topics of material fundamentals, modeling, characterization, management, applications, and market participation of Li-ion batteries to lay out an overarching theme of the management of grid-connected battery systems, serving readers and researchers as a gateway into the relevant literature. To this end, this paper is articulated, as shown in Fig. 1, in order to encapsulate all the essential topics this review is concerned with. The study also aims to outline a number of underlying challenges and potential research directions associated with grid-connected battery storage systems that the authors believe would be worthy of investigation.

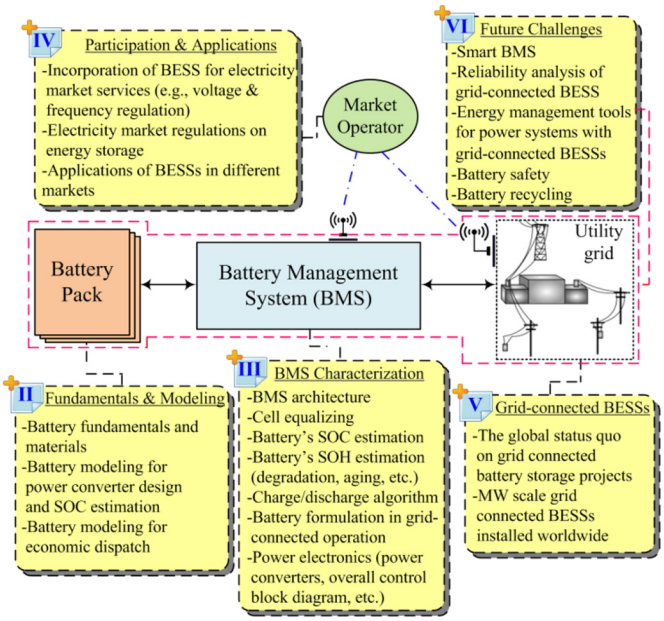

Fig. 1. The structure of the paper.

The remainder of this paper is organized as follows. Li-ion battery fundamentals and modeling are discussed and introduced in Section II. BMSs are extensively studied in Section III. Section IV discusses the participation of BESSs in electricity markets. Global battery energy storage projects are statistically discussed in Section V. In Section VI, the challenges in the implementation and management of grid-connected BESSs are reviewed. Finally, Section VII concludes the paper.

II. Battery Fundamentals Overview and Application Oriented Modeling Approaches

In this section, an overview of Li-ion battery materials is given first to provide researchers and engineers in electrical and power engineering with a glance of battery materials fundamentals. Circuit-based battery modeling is then reviewed for circuit simulation and power converter design purposes. Economic dispatch models of battery systems are also introduced for grid-connected battery storage applications.

A. An Overview of Li-Ion Battery Fundamentals

In this subsection, a brief review is conducted on the different existing and potential developments in the materials used for the anode, cathode, and electrolyte of Li-ion batteries. Determining the state of charge (SOC) of a battery through voltage measurement seems to be simple, but it can be imprecise because the terminal voltage is affected by cell materials,

charge/discharge current, and temperature. Thus, it is useful to understand how cell materials may complicate the battery's electric and thermal management.

Lithium batteries are appealing because, in the periodic table, Lithium is a very electropositive element, which also happens to be the lightest metal, half as dense as water [21]. A battery, in general, consists of in-series/parallel connected electrochemical cells. Each of the cells contains a negative electrode (anode when discharging) and a positive electrode (cathode when discharging) separated by an electrolyte layer [22]. There also exists a separator, which functions as a barrier between the cathode and anode.

Currently, carbon (graphite) is the most widely used anode material, while silicon, metal oxides, and alloyed metals are also being explored as high-capacity carbon alternatives [4], [22]–[23]. New developments have led to altered artificial graphite and altered natural graphite for anode [23]. Lithium Titanium Oxide is one of the commercialized Lithium transition metal oxides for Li-ion batteries [22]. Among the most-referred-to Li-alloy anodes is Li-Al (lithium aluminum). In addition to the aforementioned commercialized ones, the candidate materials under development for the anode would be nanostructured host materials such as Si-nanowire [4], [22].

More recent research efforts have been focused on the positive electrode, which is known as the critical component of a battery that affects its performance the most [4]. The most common cathode materials in a Li-ion battery include $LiCoO_2$, Li-Mn-O, $LiFePO_4$, and lithium layered metal oxide [24]. Lithium Manganese spinels (Li-Mn-O), whose use is still widespread, was one of the early research attempts for obtaining cathode material. Despite the reduced capacity of Li-Mn batteries due to frequent cycling, the toxicity of lithium cobalt-based materials (Li-Co-O) and costly production of lithium-nickel based (Li-Ni-O) materials are the reasons why Lithium Manganese (Li-Mn) is still popular. Lithium iron phosphate ($LiFePO_4$) batteries are of flat discharge plateau and moderate capacity ranging from 150 to 160 mAh/g. Other than being non-toxic and showing little capacity decline through the battery life, they are also safer than the Li-cobalt one, thereby making them favorable for higher power level applications [22].

The discharge voltage curves of Li-Mn and Li-phosphate are very flat. Nearly 80% of the energy stored in such batteries falls under the flat part of the voltage profile. This characteristic is desirable because it means that the voltage remains nearly constant as the battery is discharged, which simplifies the application design. However, a flat curve causes a challenge for voltage-based SOC measurement. The cell voltage measurement is less challenging with other Li-ion chemistry batteries, such as Li-Polymer and Li_2TiO_3 [1]. This shows how a material that works well for one purpose might compromise another. Taking Cobalt as an example, which is commonly used as the cathode in lithium-ion batteries, provides a high energy density, but has a limited temperature range [25].

While the anode and cathode materials govern the basic performance of a battery, electrolyte and separator are tightly associated with safety. Solid-state electrolyte is an emerging technology, which according to [26] promises lower price, rapid charging/discharging, and improved safety. When the electrolyte is polymer-based, there are only a few options from which the electrolyte can be chosen to provide the required high ion conduction due to the electrochemical stability concerns of the polymer [27]. However, the options are more diverse when the electrolyte is liquid, which can have different solvents with specific dielectric and viscosity constants [22], [28].

TABLE I
LI-ION BATTERIES WITH THREE DIFFERENT CATHODE MATERIALS [25]

Specifications	Lithium Cobalt	Lithium Manganese	Lithium Phosphate
Specific energy density (Wh/kg)	150-190	100-135	90-120
Internal resistance (mΩ)	150-300	25-75	25-50
Cycle life (80% discharge)	500-1000	500-1000	1000-2000
Fast charge time	2-4 h	1 h or less	1 h or less
Cell voltage (nominal)	3.6 V	3.8 V	3.3 V
Thermal runaway	150° C	250° C	270° C

Table I shows how the characteristics of a Li-ion battery are influenced by its cathode material. As it is shown, battery materials should be considered carefully when choosing a battery for a specific application. There is a tradeoff as different cathode, anode, and electrolyte combinations may improve one quality of the battery, but weaken another.

Ternary Lithium batteries have been developed to partly overcome the above-mentioned tradeoff. In ternary technology, the cathode is composed of a few (often three) different substances. The ratio of the constituent materials can be adjusted to reach the desired levels of cost, safety, and cell voltage. Lithium Nickel Cobalt Aluminum Oxide (NCA) and Lithium Nickel Manganese Cobalt Oxide (NMC) are two ternary technologies that are being widely used. EV application is targeted by NCA, while the use of NMC is more diverse and includes grid applications.

It is essential to note that there exist other types of electrochemical systems, such as Redox Flow Battery (RFB) [29], NaS battery [30], fuel cell-electrolyzer with hydrogen storage [31], etc., which are also suitable for grid-scale energy storage applications. RFB, for example, is a rechargeable battery whose operation is similar to fuel cells. Unlike conventional batteries, RFB does not store chemical energy at the electrodes, but in the electrolyte solutions. An important feature of flow batteries is that their power rating is a function of the geometry and size of the electrodes, whereas their energy storage capacity depends on the size of the tanks in which the electrolyte solutions are stored, thereby making the power rating and energy storage capacity of RFBs independent of one another. This feature as well as limited self-discharge characteristics cause flow batteries to be particularly useful for large-scale stationary applications, e.g., for use with sustainable but non-dispatchable wind and solar farms and for the stability (demand leveling) of the power grid. Because of the bulkiness of the electrolyte tanks of flow batteries, their application is currently limited to stationary cases. However,

TABLE II
EVALUATION OF DIFFERENT BATTERY MODELING METHODS

	Advantages	Disadvantages	Applications
Electrochemical	• High accuracy	• High computational burden • High nonlinearity • Excessive parameters	• Cell design [33]-[34], [39]
Equivalent circuit	• Balance between accuracy and complexity • Ease of online implementation	• Limited accuracy	• Estimation of battery state [40] • Energy management of new energy vehicles [41] • Grid-connected energy storage [38]
Empirical	• Low complexity due to linearity • Ease of online implementation	• Low accuracy • Lack of insight of battery dynamics	• Grid-connected energy storage [35]

another feature of the flow battery is its quick charging capability. This feature, which is currently under research, makes flow batteries suitable for frequency regulation of electric grid and even for EV applications.

B. Circuit-Based Battery Modeling

Accurate battery models are required to design, implement, and manage grid-connected BESSs. Basically, the battery models from the literature can be divided into electrochemical, equivalent-circuit, and empirical models [32]. The focus is given to electrical circuit models while the other two approaches are also briefly reviewed.

The relevant advantages and disadvantages of the aforementioned modeling approaches are shown in Table II. Electrochemical models give a deep insight into battery dynamics inside a cell during charging and discharging. The internal mass transfer processes are depicted by a series of highly nonlinear differential equations. Thus, electrochemical models can achieve very high accuracy. However, due to the high nonlinearity, high coupling and numerous parameters, it suffers from high computational burden, which makes the electrochemical models not suitable for online implementations (i.e., in energy management systems) [33]–[34]. As a black box model, empirical models mainly depict the input and output of battery energy [35]. They are often linear functions of charging and discharging power. The lower complexity makes the empirical models easy to be implemented online and contributes to the most applications in grid-connected energy storage. However, due to lack of insight of the internal battery dynamics, empirical models have the worst accuracy [36]. In the equivalent-circuit models (ECMs), a lumped-element circuit comprising resistors and capacitors represents the battery's behavior [37]. ECMs are able to maintain a balance between model complexity and accuracy so that the battery model can be embedded in microprocessors for real-time applications. ECMs are commonly adopted as they have only a few parameters to tune. They are fast to execute, simple and intuitive

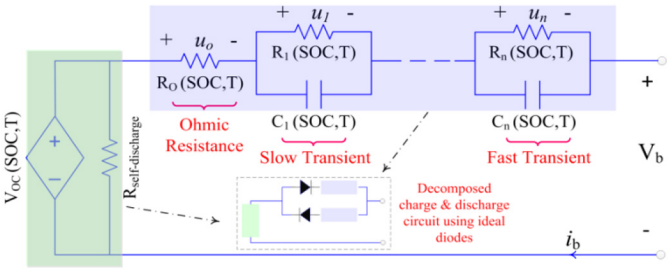

Fig. 2. The n^{th}-order ECM for a Li-ion battery.

to analyze, and, more importantly, straightforward to be integrated with other electrical models (i.e., power converters) in the system for grid-level simulations [38].

It should be noted that apart from the above-mentioned modeling methods, there also is the dynamic Kinetic Battery Model (KiBaM) for a battery, which was proposed by Manwell and McGowan [42]. KiBaM considers the battery as a two-tank system including directly available charge and bound charge to describe the charge/discharge processes. The main advantage is its capability to model the recovery and the rate-capacity effects [43]. However, KiBaM includes five sub-models (capacity, voltage, charge transfer, battery losses, and battery life sub-models) and requires the identification of a significant number of parameters [44]–[45]. Consequently, ECM will be mainly discussed in this paper due to its simplicity, effectiveness, and ease of application.

Even though Li-ion batteries are the most popular form of BESSs, a perfect Li-ion ECM is yet to be proposed to best represent its three main areas of operation that include charging, discharging, and idle modes [10]. The so-called Dual Polarization model or the Two-Time Constant (TTC) representation of the resistor-capacitor ladder circuital model (also known as Battery nth-order Randle Circuit) is the most popular battery model in the literature [38], [46]–[47]. In general, the more RC circuits are used, the better the model can capture the transients of the battery. Fig. 2 shows such a multi-time-constant ladder network; where V_{oc} is a dependent voltage source representing the open-circuit voltage (OCV), which is the battery's terminal voltage after the battery is fully relaxed and reached an equilibrium state [48]; i_b is the terminal current; V_b is the terminal voltage; and R_o is the ohmic resistance.R_o is responsible for the instantaneous voltage drop/rise in the battery response [49]. R_1 to R_n are the leakage [50] or transient resistances, and C_1 to C_n are the corresponding dynamic capacitances.

In a TTC model, the elements R_1 (Charge-Transfer Resistance), C_1 (Double-Layer Capacitance), R_2 (Diffusion Resistance), and C_2 (Diffusion Capacitance) [32] would represent two RC branches that model the corresponding long and short time constants of a battery's step response, respectively [51]. The duration of the slow transient response is in the order of hours [38]. R_1 to R_n and R_o strongly depend on temperature [52]. $R_{self-discharge}$ denotes the self-discharge energy loss when batteries are stored for a long time. It can be considered to be a large resistor or even ignored [53]. As seen from Fig. 2, besides $R_{self-discharge}$ all

the other circuit parameters are non-linear and functions of the battery's SOC and operating temperature. It is notable that the purpose of using ideal diodes shown in Fig. 2 is to make the model possess different parameters during the charge and discharge operations, which would provide further freedom degrees when estimating the ECM parameters. In addition to the circuit shown in Fig. 2, there also exists the ADVISOR model. Further details on this model can be found in [54].

The circuit parameters of Fig. 2 are, in general, non-linear multivariable functions of the SOC and temperature (as well as aging, current direction, and charge rate [32]). Since these detailed data are not given in the battery's datasheets, these parameters have to be estimated [55]. The parameterization of a single-RC equivalent circuit would be straightforward. However, the lack of systematic parameter identification methods for multiple-RC equivalent circuits has led to the use of ad hoc methods and iterative numerical optimization techniques [32]. These parameter identification approaches can be split into two main categories: the frequency domain (impedance spectroscopy) and the time domain method, both to minimize the difference between the actual voltage measured at the battery terminals and the one estimated by the equivalent circuit [37]. In the former, the battery is excited with a small voltage/current signal over a range of frequencies (from Hz to kHz). The impedance of the battery is then analyzed over that frequency range. The simple principle used in this method is that at low frequencies, the impedance is the sum of the resistors, and at high frequencies the impedance corresponds to R_o [37] (see Fig. 2). Although the technique can accurately represent the battery characteristics, this method's online implementation is considered cumbersome, as it involves additional and complex circuitry [56]. Unlike the former method, the time domain method is attractive, as it requires no impedance measurements [57]. In the time domain method, the battery is excited with a discharge (or charge) impulse current, as shown in Fig. 3, to detect the internal resistance as well as the time constants of the charge transfer and diffusion phenomena [37].

The main challenge in both the two aforementioned methods is the fact that resistance and capacitance parameters are not constant but vary as the operating conditions, such as temperature and SOC, change [56]. Both SOC detection and parameter identification of the equivalent circuit still remain two ongoing discussions [32]. Another research question that is not fully investigated yet is the effect of temperature on the equivalent circuit parameters [48]. It is essential to note that the inaccuracies of the ECM pop up when the battery is cycled with C-rates different from the ones used to infer the equivalent circuit parameters [48].

In addition to the battery model we discussed above, which is known as the integer-order model (IOM), there is the fractional-order model (FOM) proposed to better capture the dynamics of a battery. An IOM may capture a battery's behavior to a moderate degree of accuracy within a limited range of operating conditions [58]. IOMs are commonly incapable of predicting a battery's dynamics in both the time and frequency domains over the entire operating range. In IOMs, the more RC branches are added, the greater the accuracy would be.

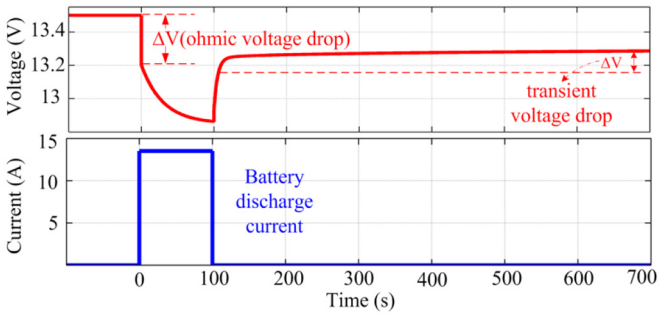

Fig. 3. Typical Li-ion battery response under a pulse discharge current.

However, this not only complicates the model mathematical structure associated with computational burden, but also increases the effort required for system calibration as well as the risk of over-fitting. The impedance spectrum of a Li-ion cell can be divided into three parts: the low-frequency straight line, the mid-frequency semi-circle, and the high-frequency tail. The impedance spectrum of a Li-ion cell is commonly plotted using the Nyquist plot, and the phase shift decides the slope of the straight line and the shape of the semicircle. In FOM, there is a fractional element that possesses a phase shift of $\alpha\pi/2$ $(0 < \alpha < 1)$, and it is used to replace the pure capacitor in IOM. Using the FOM, the mid-frequency response that reflects the lithium diffusion within electrodes can be captured more accurately. In other words, FOM provides an infinite-dimensional model for Li-ion cells [59]–[60]. Therefore, the accuracy of FOM is higher than IOM.

C. Modeling a Battery System for Economic Dispatch

The cost function of battery storage systems is not as readily available as the generation cost curve of conventional generators. The main cost of a battery system is its investment cost. Levelized cost of energy (LCOE in $/kWh) is commonly used to account for a battery's operation cost [61]. In addition to the energy cost, there is battery degradation that may be added to the aforesaid operation cost of a battery [61]. A precise battery economic dispatch model not only updates the cost of stored energy by keeping track of the charge/discharge history but also takes into account the impact of the age and charge/discharge on the battery capacity [62]. Thus, there is a big motivation to develop a model to estimate the capacity fade for one dispatch period as a function of exchanged power, dispatch time interval, and SOC change [61]. Clearly, finding a model analogous to the fuel cost function of thermal generators is appealing. Such a sought-after battery operational cost model is divided into an electrical and a degradation model. Most of the research efforts in the literature have been focused on the degradation model as the electrical part (i.e., the equivalent circuit) is relatively well known. The initial SOC and the power to be dispatched are given to the electrical model to receive the updated SOC. The data is then given to the battery degradation model to get the per-unit-energy degradation cost. The degradation models introduced in the literature [60]–[61] depend on the application and chemistry

of the battery. For example, [63] proposed (1) as the degradation model of $LiFePO_4$ batteries when used for secondary reserve provision.

$$Q_F(d, T, SOC) = \left(\beta_1.SOC^{\beta_2} + \beta_3\right).\left(\beta_4.T^{\beta_5}. + \beta_6\right).d^{\beta_7} \quad (1)$$

where, Q_F denotes capacity fade in percentage, β_1 to β_7 are fitting parameters, T is the temperature, and d is the time duration in months. Equation (2), which is a quadratic relationship between the depth of discharge (DOD) and degradation, was proposed by [64] for distribution-sited Li-ion batteries.

$$\Delta Q_F = k \times DOD^2 \quad (2)$$

where ΔQ_F is the capacity degradation per cycle. The coefficient k is set at a value such that (2) best fits the experimental measurements. The implementation of (2) is less challenging than (1) as it maintains compatibility with larger economic dispatch models, which often are quadratic. Additionally, (2) can be more easily linearized using mixed-integer techniques if needed.

In addition to [63]–[61], [64]–[62] and [65]–[68] also aimed to propose a dispatch model for batteries. A battery economic dispatch with time-coupling constraints was given in [65], and a generic dispatch model was suggested in [66]. The study sees the storage as an energy reservoir, but it does not account for the degradation. Reference [67] investigated the opportunity costs hidden in the dispatching of battery storage systems when accompanied by controllable generators. The use of Model Predictive Control (MPC) for optimal battery dispatch has also been attempted [63]. Because power system operation models are often linear, efforts have been made to come up with a linearized battery cost model [69]. Further battery cost models can be found in [70]–[72].

It should be mentioned that the development of a comprehensive battery cost function that captures all the factors involved in the degradation is still under debate, which stems from the lack of an all-inclusive definition for the state of health (SOH) of a battery. The topics of degradation and SOH are tightly dependent and will be extensively discussed in Section III.

III. Management of Grid-Connected BESSs

Utility engineers will soon need to be familiar with the BMS, shown in Fig. 4. A BMS is required to perform SOC/SOH estimation, thermal management, balancing, monitoring, and control at the cell, module, and pack levels. These features are available if the BMS is well designed in circuit and possesses accurate algorithms to measure/estimate the functional status of the battery. A BMS consists of numerous embedded sensors, actuators, controllers, and signal lines. The major motivation of a BMS is to maintain the safe operation of a battery pack and prolong the battery pack's useful life. Achieving such a BMS would significantly escalate the growth of grid-connected BESSs [1]. The features expected from a BMS are discussed as follows.

A. Cell Balancing

The mismatch of voltage and capacity among the cells in a battery pack introduces challenges in battery management,

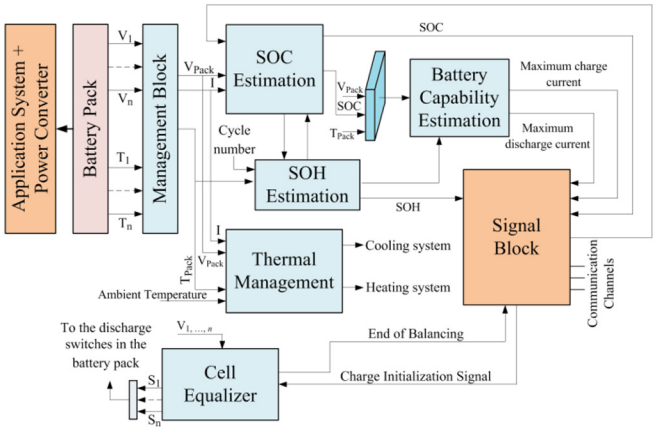

Fig. 4. Block diagram of BMS.

reduces storage capacity utilization, and may accelerate battery degradation if not well managed. In most used battery power electronic architectures, the BMS entirely stops the discharge once the very first cell reaches its cutoff voltage, thereby making the energy in the rest of the cells inaccessible. Likewise, the BMS may stop charging once the cell with the highest SOC is fully charged, whereas other cells have not been fully charged yet. Thus, after several charge/discharge cycles, the battery strings tend to go out of balance. Such a mismatch stems from an inconsistency in either the cells' capacities or the cells' SOCs due to manufacturing tolerances (intrinsic) and varying ambient conditions (extrinsic) [73]–[74]. Therefore, it is important that a BMS be equipped with cell balancing capability. Cell balancing techniques are divided into passive and active. The passive cell balancing is easy to implement as it requires only a control switch and a shunt resistor in each cell to dissipate the extra charge in heat. Whereas active cell balancing moves the extra charge to the less charged cells using dc-dc converters [75] or bypassing [76] the overcharged (undercharged) cells during the charging (discharging) process, respectively. Unlike the passive technique that suffers from high losses and thermal issues, the active approach is more efficient. The active balancing techniques vary in the strategy used to redistribute the extra energy among the cells. However, a compromise between the complexity of the active balancing circuit and the achievable efficiency must be made to make active balancing competitive against the passive one. The active balancing circuits are split into switch-cap-based [77] and inductor-based topologies [75]. Although relatively slow, the capacitive topology is of simple control algorithm, high power density, less electromagnetic interference (EMI), and is well-suited for on-board integration. However, the shortcoming is that the switch-cap-based topology becomes less efficient when it comes to batteries with a considerable number of series-connected cells as the balancing charge would have to travel through the long cell strings. That is why it is occasionally preferred to use the counterpart (i.e., inductive topology), which is subcategorized into non-isolated [78]–[79] and isolated balancing circuits [75]–[77], each of which has its own pertaining pros and cons.

High energy transfer is an issue when SOC balancing is performed at the module level. An ideal solution to the issue

is to charge low SOC modules with an external energy source such as a PV panel (solar harvesting) [80]. In such a solar-assisted battery balancing system, the SOC/voltage of the battery modules is monitored, and then the module with the lowest SOC/voltage is connected to the PV. When all the battery modules are equalized, the whole battery pack can be charged by the PV via a buck-boost converter.

It is worth noting although passive balancing is less efficient, it is often preferred as it is less costly and easier to implement [81]. Hybrid passive-active techniques and smart batteries have also been suggested as solutions to the present struggles in cell balancing [19], [82].

B. Thermal Management

Li-ion batteries best perform when kept at a specific temperature range (for example, 15-35 °C [83]). If overheated (for example, above 100 °C [84]) due to short circuit or fast charging/discharging, a Li-ion battery may undergo a catastrophic cascaded thermal runaway or even an explosion. The IEEE standard [85] defines this thermal runaway as: "A condition that is caused by a battery charging current or another process that produces more internal heat than the battery can dissipate." Most of the present challenges in a Li-ion battery are somehow associated with thermal issues [86]. Thermal and SOC imbalances are the two well-known causes of early battery aging [87]. Thermal imbalances are sourced by the manufacturing variations and temperature gradient in the coolant [88]. Therefore, a thermal management model, which can be easily integrated into the BMS, is required to identify the temperature spatiotemporal distribution in the battery and choose a proper heat-dissipating strategy. In [86], Bernardi mathematically formulated the thermal behavior of batteries and introduced a heat generation formula that can be defined by (3).

$$\dot{q} = I\left(U - V - T\frac{\partial U}{\partial T}\right) \tag{3}$$

where $\dot{q}$ is the heat generation rate, I and T represent the current and temperature, respectively. U is the open circuit potential, and V is known as the working voltage. The use of (3) to estimate battery heat generation is quite widespread. However, the equation assumes that the current is uniformly distributed throughout the battery, which is not true for large batteries. Thus, Pals and Newman, [86], proposed a one-dimensional lumped model to predict the thermal behavior of a Lithium battery cell. The lumped thermal model is very simple, and thus, convenient to be used in BMS applications.

Depending on what coolant is used in the battery, the thermal management is grouped into: 1) air cooling, 2) liquid cooling, 3) phase change materials (PCM), and 4) heat pipe [89]. The air cooling is simple and inexpensive. Liquid cooling is split into indirect and direct (immersion) cooling. In the indirect, the coolant is in a looped circulation and not directly in contact with the cells. Many EV manufacturers, such as GM and Tesla, use indirect cooling. In direct cooling, the entire surface of the cell is immersed in a liquid of high enough dielectric strength [83]. Compared to the air, direct-contact liquids are of a much better heat transfer rate. Indirect-contact liquids (i.e., water or water/glycol solutions) might perform three times better than that of air cooling [89]. The heat pipe, which is used widely in electronic devices and scarcely in commercially-available battery packs, is a heat-transfer device that takes advantage of thermal conductivity and phase transition and gives a highly-efficient heat transfer between two solid interfaces [89]. PCM is a material of great potential for heat absorption with minimum volume change but has low thermal conductivity (0.17 – 0.35 W/mK at room temperature [90]).

PCMs store the battery's heat rather than transfer it outside the battery pack [90]. The use of PCM eliminates the need for any additional cooling system, whereas the heat pipe will have to be accompanied by air or liquid cooling [89]. Despite the aforementioned advantages of liquid, heat pipe, and PCM cooling, compelled air circulation remains the most functional cooling system for battery packs because of its low cost and weight [91]. Air cooling is also essential for battery packs that may produce dangerous gasses [91].

As thermal and cell balancing are two tightly interdependent objectives, [92] proposes a simultaneous thermal and SOC balancing approach through non-uniform use of cells. The approach adopts active balancing as it is more thermo-friendly than passive balancing. The design of a cooling system is remarkably impacted by the geometry (shape and size) of battery cells [93]. Fluid dynamics have been extensively studied to optimize cooling systems [89]. Proactive thermal management for early warning and timely detection of thermal runaway by using prediction techniques has also been tried [89]. Discharging the stored energy often is a proper protection tactic to avoid a thermal runaway [89]. Graphene-enhanced PCM for conductivity improvement as well as a model development for online spatiotemporal temperature estimation with few measuring sensors have also been investigated in the literature [90].

C. SOC Estimation

SOC is indicative of the actual charge stored in a battery relative to its full capacity charge. Precisely knowing the SOC is imperative for the management and control of battery packs because SOC is involved in various functions offered by a BMS. However, this parameter cannot be directly measured at the battery terminals. Algorithms are needed to accurately estimate the SOC of the battery pack and the individual cells based on the measured data of each one. Different algorithms and approaches have been proposed in the literature to estimate the SOC from the battery's obtainable measurements. Coulomb counting is probably the most classical one in which the battery's terminal current is integrated over time to compute the battery's incumbent charge [94]. Since the current is integrated over time to compute the residual charge, the current sensor has to be of no offset over the temperature and time. In this method, the SOC is calculated by (4) [95], in which η is the Coulomb efficiency, Q_{batt} is the battery's rated capacity in Ampere-hour (Ah), I_{batt} is the battery's discharge current in Ampere, and $SOC(t_0)$ is the battery initial SOC.

$$SOC(t) = SOC(t_0) - \int_{t_0}^{t} \frac{\eta I_{batt}(\tau)}{3600 Q_{batt}} d\tau \tag{4}$$

The unknown initial SOC, the need for perpetual current acquisition, and the current sensor error, which adds up over time because of the integration process, are the three major challenges in this method though it is straightforward to implement. Therefore, measuring the OCV has been suggested as an alternate method to compute the SOC given the static relationship (i.e., a lookup table) between the OCV and the SOC. But, the measurement of the OCV requires the battery to be at rest. That is, the battery needs to be fully disconnected from the system. Due to the very slow dynamics in a battery, measuring the OCV can be time-consuming up to even eight hours, making this method impossible for online applications though it still can be used for laboratory tests and calibrating. Thus, some research efforts have investigated fast OCV predictions [47] without waiting for the battery to reach a steady state. The study proposes a fast approach based on exponential recovery voltage. In this approach, only three voltage measurements are required during the recovery process. The OCV is then predicted from a quadratic equation.

Electrochemical impedance spectroscopy (EIS) can be considered as another lookup table method by establishing the relationship between the SOC and battery electrochemical impedance spectrum [96]. Although EIS is a proper testing method for SOC, it is difficult to be used in practical battery management systems.

Reference [97] showed that some of the battery model parameters might change as much as 800% when the SOC changes from 0 to 100% while the temperature and charge rate are kept constant. To overcome this issue, parameters-SOC co-estimation was proposed in [1], [97]–[98]. Reference [99] proposes a joint battery model and SOC estimation method based on the sigma point Kalman filter (SPKF). In [100], a single-parameter tuning approach within an extended Kalman filter (EKF) was used to find an observer with straightforward tuning for simultaneous estimation of the battery's parameters and SOC. The use of H-infinity filters for joint estimation under uncertainty has been also tried [20]. The study estimates the battery parameters online using the H-infinity filter, and the SOC is then estimated using the unscented Kalman filter.

More recent research efforts have moved toward nonlinear observers (NLOs) and machine learning based algorithms [101]–[102]. In addition to Kalman filter (KF) based methods, NLOs have also been extensively studied for SOC estimation, such as SOC-dependent gain matrix based nonlinear observer [103], the statistical filter algorithm (SFA) [104], sliding mode observer (SMO) [105]–[107], Luenberger observation [108], etc. Compared with Kalman filter based algorithms, nonlinear observers have strong robustness to nonlinear features with less computation cost. Various intelligent learning and/or data-driven approaches [109], such as neural network (NN) [110]–[111], fuzzy logic [112], fuzzy-neuro [113], and supporting vector machine (SVM) [114]–[115], have been proposed for improving the accuracy of SOC estimation. In this category, the battery system is normally treated as a black or gray box. The learning algorithm will learn the relationship between the input data (battery voltage, current, charge/discharge rate, temperature, etc.) and the output quantity (e.g., the SOC).

TABLE III
BATTERY SOC ESTIMATION METHODS

Direct Methods	Coulomb counting	Simple but with accumulation errors and dependent on initial SOC value
	Lookup table • OCV • EIS	OCV: Simple but with long testing time to measure OCV and hysteresis effect; EIS: High accuracy but not suitable for online battery management
Kalman Filter Based Methods	KF EKF SPKF Other KF based methods	Good accuracy with the capability of handling nonlinearity for KF variants; Dependency on the battery model accuracy and having issues of robustness
Nonlinear Observers	NLO SFA SMO	Improved accuracy and converge speed with reduced computation cost; Issues in finding a proper gain matrix to reduce the error and in tuning the switching gain to control sliding regime for SMO
Intelligent Learning Algorithms	NN Fuzzy Logic SVM	No need for battery models. High capability in handling nonlinearity with good accuracy in SOC estimation. Good training data is required, and the computation cost is high.

A summary of various SOC estimation methods is given in Table III. For a detailed comparison of SOC estimation methods, readers are referred to [101]–[102].

D. SOH Estimation

Unlike SOC, whose definition is well agreed upon, there is not a precise definition for SOH [116], which is difficult to determine and impacted by various factors [117]. Equation (5) [117] represents the estimation of SOH based on capacity degradation (i.e., Q_F). Q_{batt} is the battery capacity at the beginning of its life.

$$SOH = \frac{Q_{batt} - Q_F}{Q_{batt}} \times 100 \tag{5}$$

As seen from (5), it is the battery degradation that needs to be defined first. In order to select cells of equal capacity for battery pack assembly or to tell if an aged battery pack is worth being reused, it is important to know the actual capacity of battery units. The capacity of a Li-ion battery degrades as it ages. The loss of active material at the anode and cathode, the loss of lithium inventory, and the increment of total polarization potential are among the main causes of the degradation [118]. From the perspective of battery management, the degradation is divided into two types, calendric and cyclic aging. Calendar aging is often reported as a function of storage conditions [119] (e.g., temperature and SOC), whereas the latter depends on the depth and frequency of charge/discharge cycles [120]. The battery materials also play a key role in the degradation [119]. Although the self-discharge of Li-ion batteries is relatively low, the impact of calendric aging is often more significant than cyclic aging for stationary applications [121]. However, the calendric degradation is minimal when short-term operation is considered.

A basic equation to represent the capacity fade due to calendric aging would be as defined in (6) [122]. The model

formulates the degradation as a function of time, SOC, and temperature.

$$Q_{F,cal}(t, SOC, T) = \alpha e^{-(\beta t+1)} + \gamma t + 1 \tag{6}$$

where $Q_{F,cal}$ represents capacity fade, t is time, and T is the temperature. α, β, and γ are fitting parameters whose values depend on SOC and temperature.

As the dependence of calendric aging on the battery's internal resistance increase has been well studied and quantified, [123] suggested (7) for computing the resistance increase of lithium iron phosphate batteries.

$$R_i(t, SOC, T) = k.e^{(a.T)}.e^{(b.SOC)}.t^c \tag{7}$$

where, R_i is the internal resistance increase expressed in percent, t is time expressed in months, and T is the temperature in Kelvin. The values of a, b, and c, which are positive, are given in [123]. In general, calendric capacity fade is larger at higher SOC and temperature as also seen from (7). Further calendric aging models can be found in [124].

The capacity fade due to cyclic aging can be calculated by using (8) [125].

$$Q_{F,cyc} = A_{DoD}.e^{\left(\frac{E_a}{RT}\right)}.N^Z \tag{8}$$

where $Q_{F,cyc}$ is the capacity loss due to cycling. A_{DoD}, E_a, R, T, N are pre-exponential factors, activation energy, gas constant, operation temperature, and number of cycles, respectively. A_{DoD}, E_a, and Z (cycle exponent) depend on the battery characteristics, and need to be obtained from the battery's datasheet using curve fitting techniques [125].

It is notable that, in addition to the aforementioned causes for degradation, the current ripple caused by batteries' power electronics converters, depending on their switching frequency, may contribute to the battery degradation as well [126]. To evaluate the cumulative impact from all the cycles, a rainflow counting algorithm is often used. The rainflow algorithm has been extensively used in the analysis of fatigue data, including battery life assessment [127]–[128].

As mentioned earlier, there is not a well-agreed-upon quantitative index to compute SOH, and thus, different methods have been suggested. For instance, [129] suggests (9), which is based on the change rate of the battery's internal resistance.

$$SOH = \frac{R_{end} - R_{current}}{R_{end} - R_{new}} \times 100 \tag{9}$$

Reference [130] suggests computing both (5) and (9) and then choosing the smaller one to stay conservative about SOH. According to [117], the end of life (EOL) of batteries is denoted as 20% capacity degradation or doubling of the internal resistance though there is no strong proof to verify these claims.

According to [131], the methods for estimating SOH can be grouped into: 1) physicochemical aging model, 2) event-oriented aging model, and 3) weighted Ah throughput aging model. The third one estimates SOH with better precision and computational complexity than (5) and (9), and has been used for reliability evaluation of battery systems. Under constant operating conditions, the model assumes that a battery can provide a certain amount of energy throughput, equivalent to a number of charge/discharge cycles, before its EOL is reached. This model suggests (10) to calculate the SOH of a battery module (cell) in the i^{th} operating condition [131]:

$$SOH_i = SOH(0) - \frac{\int_0^t |P_{B,i}(\tau)|.d\tau}{2N_{equ,i}.Q_{batt}} \tag{10}$$

where $SOH(0)$ represents the initial SOH of the battery module (cell); $SOH(0)$ is 1 for a brand new battery module (cell). Q_{batt} is the initial battery module capacity in kWh; $P_{B,i}$ is the battery module power during the i^{th} charge/discharge cycle (or operating condition); $N_{equ,i}$ is the equivalent number of charge/discharge cycles before EOL under the i^{th} operating condition and is not a constant number but a variable as defined by (11).

$$N_{equ,i}\left(C_{rate,i}\right) = \frac{U_B.Ah_i\left(C_{rate,i}\right)}{Q_{batt}} \tag{11}$$

where $C_{rate,i}$ is the C-rate under the i^{th} operation condition; U_B is the OCV of the battery module (cell); and $Ah_i(C_{rate,i})$ is the total charge throughput under the i^{th} operating condition. Assuming the capacity fade (i.e., Q_F) is available, $Ah_i(C_{rate,i})$ can be found using (12).

$$\Delta Q_F = B.e^{\left(\frac{370.3\times C_{rate,i}-31700}{RT}\right)}.\left(Ah_i\left(C_{rate,i}\right)\right)^z \tag{12}$$

where ΔQ_F is the percentage capacity loss with respect to the initial capacity. B is the pre-exponential factor and can be found in [132]. R is the gas constant, which is equal to 8.31 J/mol.K; T is the absolute temperature; and z is a constant factor, which is equal to 0.55 for lithium-ion batteries.

Experimental measurement has revealed that capacity delivery is enhanced by connecting cells with similar SOH in series. This has recently led to developing algorithms for SOH-aware reconfiguration of battery cells and also manufacturing fully reconfigurable batteries [133]. State of function (SOF) [117] and remaining useful life (RUL) [12] are two other indices that function similarly to SOH. The SOF of a battery represents the ability of a battery to support a specific application in its present state [117]. RUL is usually defined as the number of charge/discharge cycles remaining until a failure threshold is met [134]. It has been claimed that these indices (i.e., SOC, SOH, SOF, and RUL) should be co-estimated as they are tightly correlated [134].

An experimental study [119] over the grid-connected 250 kW/500 kWh Li-ion battery storage facility in Qatar showed that the residual capacity of the system was around 93% of its initial capacity after three years of storage at high SOC.

Similar to SOC estimation, machine learning methods have also been investigated for battery SOH estimation [135]. Machine learning (or data-driven) approaches do not require a sophisticated battery degradation model. Real battery testing data are used for training the algorithm to predict battery degradation level and SOH. A variety of learning algorithms have been reported for SOH estimation, including NN based methods [136], fuzzy logic [137]–[138], extreme learning machine (ELM) [139], support vector regression (SVR)/SVM

TABLE IV
BATTERY SOH ESTIMATION METHODS

Experimental Methods	Internal R EIS Energy/capacity	Direct and simple with reasonable accuracy. Not suitable for actual battery management.
Degradation Model Based Methods	Physicochemical Event-oriented Ah throughput	Fast and accurate if the model is validated. Model validation is challenging. Historical data is needed.
Kalman Filter and Nonlinear Observer Based Methods	KF and KF variants SMO	Reasonably accurate with error bound estimation. Improved KF variants can handle nonlinearity but with increased computation complexity.
Intelligent Learning Algorithms	NN Fuzzy Logic SVR/SVM	No need for battery degradation models. High capability in handling nonlinearity with good accuracy in SOH estimation. High quality training data in diversity and quantity is required, and the computation cost is high.

based algorithms [140], and semi-supervised transfer learning method [141].

Table IV gives a quick summary of different SOH estimation methods. More detailed comparison and reviews of SOH estimation can be found in [18] and [142].

E. Charge/Discharge Regime

Different batteries have different restrictions on the rate at which they can be charged and discharged. The BMS on the battery pack needs to have a built-in feature to manage, optimize, and protect the charge/charging regime. In the following, conventional battery charge/discharge procedures are briefly presented, and then, it is discussed what constraints must be met when operating a grid-connected battery system.

Any charge controller involves a charging algorithm and the circuit to implement the algorithm. There are two common algorithms for battery charging: pulse charging and constant-current constant-voltage (CCCV) algorithms [143]. The former is more popular as it is simple and cheap. However, it has a major issue: the current pulse is quite high and often causes spikes in the battery voltage, which can be seriously hazardous in Li-ion batteries [144]. The latter charging strategy is done over three phases. In the first phase, known as the trickle-charge phase, the battery is tested to see if it is healthy and operating properly. This is done by observing the battery voltage slope while the battery is being injected with a constant charging current (often limited to 10 percent of the full charging current) for a preset time interval. After it is known that the battery is working properly, the second charging phase kicks in. Otherwise, the charging process is terminated. In the second phase, known as the constant-current phase, the magnitude of the charging current already applied to the battery is raised up to the full charging current and then is kept constant. The process goes on until the voltage of the battery comes to the rated value, which often corresponds to nearly 70% of the battery capacity. In this case, if the constant-current injection continued, the battery voltage would go beyond its rated level, which would damage the battery. Thus, the constant-current phase terminates at this point, and the next phase initiates. In the third phase, known as the constant-voltage phase, a certain voltage is applied to the battery, which equals the rated maximum voltage of the battery. In this phase, the charging current changes and becomes smaller and smaller as the battery voltage approaches the preset value. In other words, the battery's current gradually declines as the battery receives further charges. When the current reduces to the trickle-charging value, the constant-voltage phase ends as the battery is now fully charged [144].

The discharge procedure, which is basically current or power-based control, is often simpler than the charge procedure. The discharge is allowed as long as the battery SOC is above a certain limit and the discharge power, which is demanded by the grid, does not violate the limitations of the battery or its power electronic converter.

The overall formulation of a battery in grid-connected operation can be presented as below [145].

$$-u_t^d.\overline{P}_d^B \le P_t^B \le u_t^c.\overline{P}_c^B \tag{13}$$

$$\left|P_t^B - P_{t-\Delta t}^B\right| \le \Delta P_{Max}^B \tag{14}$$

$$E_{t+\Delta t}^B = \beta_{sd}E_t^B + u_t^c P_t^B \Delta t \eta^c + u_t^d\ P_t^B \Delta t/\eta^d \tag{15}$$

$$E_{Min}^B \le E_t^B \le E_{Max}^B \tag{16}$$

$$u_t^c + u_t^d \le 1\ u_t^c, u_t^d \in \{0, 1\} \tag{17}$$

where $\overline{P}_c^B$ and $\overline{P}_d^B$ are positive values denoting the maximum permissible charge and discharge powers of the battery, respectively. Constraint (13) causes the power flowing to the battery (i.e., P_t^B) to remain within its permissible bounds as stated by the battery manufacturer. The power variation of the battery is contained by (14) to avoid possible damages. Equation (15) gives the battery's updated energy level. In (15), the parameters β_{sd}, η^c, and η^d are the battery self-discharge, charge, and discharge efficiencies, respectively [145]. Constraint (16) ensures that the battery energy level remains within the desired range. u_t^c and u_t^d are auxiliary binary variables for charging and discharging at time t. As seen, the binary variables will lead to a mixed-integer (i.e., non-convex) model, which is computationally challenging to be solved. This challenge, as well as the motivation for real-time control of power systems, has recently led to research efforts to sidestep the non-convex constraints and propose integer-free battery operation models [146].

F. Power Electronics

Regardless of their applications and auxiliary functions, grid-connected power converters (GCPCs) need to have a few basic functions, including grid synchronization (AC voltage, frequency, and phase angle control), DC voltage control, and grid current control. The secondary level of capabilities comprises the application-oriented functions such as maximum power point tracking in PV systems, the anti-islanding, switching between grid-forming and grid-feeding modes, the fault ride through (FRT) function (the capability of staying connected during a grid disturbance event), and the grid support functions (e.g., power quality control) [147]–[151]. When it comes to BESSs, the GCPC has to be capable of some additional functions such as bidirectional power flow control, charging/discharging in voltage or current control mode,

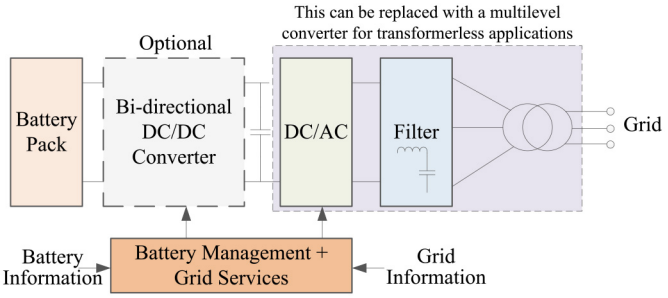

Fig. 5. A typical BESS with power electronic converters.

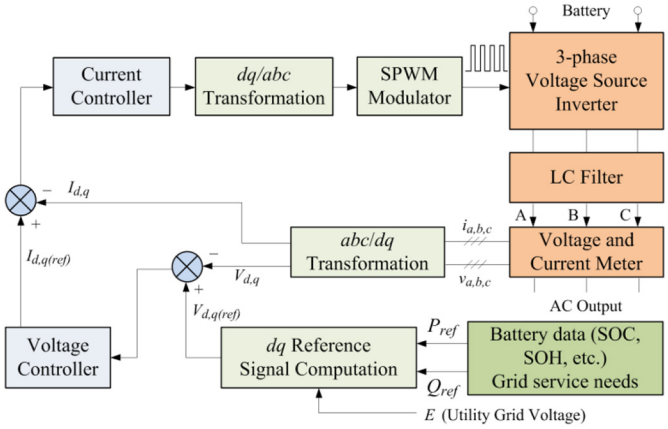

Fig. 6. Control of a grid-connected BESS via an inverter.

dynamic reactive power control, virtual generator control, frequency regulation, integrating renewable energy sources, smoothing intermittency, ramping and load following, time shifting, and blackstart function. Fault-tolerant operation of battery storage systems is also of great importance. In a fault-tolerant GCPC, a faulty module can be bypassed [147].

A conventional GCPC for BESS applications may just consist of a simple two-level (2L) converter with a line frequency transformer, as shown in Fig. 5. Topologies to substitute the 2L converter are the three-level (3L) neutral-point clamped (NPC) converter [149]–[150], the active NPC converter, and the 3L flying capacitor converter. A few four- and five-level converters have also been suggested [151]–[152]. Although the control design and modulation techniques for 4L and 5L converters are more sophisticated than for the conventional 2L converter, they provide an extra degree of freedom to increase the converter's output voltage magnitude and reduce harmonic distortion. There is a compromise for different types of multi-level monolithic converters between the increased power rating, mechanical complexity, and harmonic performance. The line-frequency transformer used in the above-mentioned multi-level converters is bulky, dissipative, and expensive. Thus, directly tied GCPCs have been proposed to avoid using a line-frequency transformer. They are divided into: 1) series-connected semiconductors and 2) series-connected sub-modules (SMs). The SMs gain from cascaded modular converters made of a basic power converter block (known as a bridge). The series-connected SMs are subcategorized into Cascaded H-Bridge Converter (CHB) and Modular Multilevel Converter (MMC). The overall control block diagram of a typical grid-connected BESS is shown in Fig. 6. The dual loop control is done in the *dq*-frame via the *abc/dq* and its inverse transformation. The battery information data such as SOC and SOH and the grid service signals are used to generate the reference real and reactive powers (P_{ref} and Q_{ref}), which can be positive (discharging) or negative (charging), to control the battery pack via the interface inverter.

In conventional power converter configurations, the converter's dc-link voltage is the voltage of the battery string whose magnitude varies depending on the SOC. Thereby, the converter is subjected to voltage variations. Thus, the design, from the perspective of semiconductor selection, may not be best optimized because the voltage rating of semiconductor elements would have to be chosen a bit over-designed. Therefore, a dc-dc converter between the battery string and the dc-link of the grid-connected converter can be added to build a controllable dc-link [13].

TABLE V
POWER ELECTRONIC CONVERTERS IN BESS APPLICATIONS

Bi-directional dc/ac converters	Transformer connected	2-level converters 3-level converters: Neutral-point clamped (NPC) converters Active NPC (ANPC) converters Flying capacitor converters 4-level and higher level converters 4L-NPC 4L-Nested neutral point clamped (4L-NNPC) converter 4L- hybrid neutral point clamped (4L-HNPC)
	Transformerless	Modular Multilevel Converter (MMC) Cascaded H-Bridge Converter (CHB) Hierarchical cascaded multilevel converter (HCMC)
Bi-directional dc/dc converters	Controllable dc-link	Boost converter Dual-active bridge (DAB) Interleaved dc-dc converters

Typical converters used for BESSs are given in Table V. DC-DC converters are also listed in the table when a controllable dc-link is needed. It should be noted that, for the sake of brevity, only representative power electronic converters for BESSs are reviewed. More details and comprehensive reviews on power converters can be found in [13] and [153].

IV. PARTICIPATION OF BESSS IN ELECTRICITY MARKETS

BESSs need to actively participate in electricity markets to not only realize various functions and services such as capacity reserve and frequency/voltage regulation that they can provide but also to compensate for their relatively high initial investment costs.

A. *Incorporation of BESS for Electricity Market Services*

For primary frequency regulation, the system frequency signal is necessary. In 2009, PJM developed RegD signal associated with the frequency deviation component of area control error (ACE) specifically for energy storage systems [154].

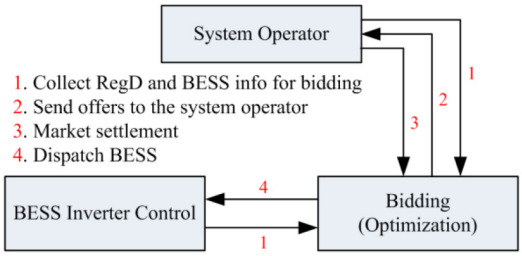

Fig. 7. BESS participation in the frequency regulation market.

With this signal, a BESS can respond to the signal and provide frequency support. If an entity has multiple BESSs, coordination is necessary. This usually involves solving an optimization problem to maximize the benefit while considering the BESS constraints, including SOC limit and aging as previously discussed. For example, optimization strategies have been proposed [128], [155] to find battery dispatch over multiple horizons (each horizon is an hour) while considering the temporal constraints of battery's energy capacity. The BESS participant submits a regulation offer to the system operator. The system operator settles the market, and the participant receives the instruction to change battery dispatch. The BESS then changes the dispatch command, to which the inverter control will respond. This interaction is shown in Fig. 7.

The frequency response to a supply-demand imbalance in a system with incorporated BESSs is governed as defined by (18) [95].

$$\frac{df}{dt} = \frac{f_{ref}}{H_{BESS} + 2\sum H_n} \overbrace{(P_G - P_L)}^{\Delta P_d} \tag{18}$$

where, P_G is the generated power, P_L is the load power demand, ΔP_d is the change in power demand, $\sum H_n$ is the total system inertia from all rotating machines, H_{BESS} is the battery system inertia constant [95], and f_{ref} is the nominal frequency.

The most common frequency and voltage control schemes have been based on the droop principle in which generation active and reactive power outputs are adjusted proportionally to the local frequency and voltage deviations [156]. Unlike conventional reserve, a BESS is energy constrained, and may fail to provide regulation service if its SOC threshold is reached. Thus, BESSs must restore their SOCs to a desired level during idle time (e.g., when the system frequency is within the dead band) to be prepared for the next upcoming event [157]. There have been attempts to devise SOC-feedback and SOC-adaptive droop control strategies for BESSs [95], [158]–[159]. For distributed energy storage systems at the distribution level or in microgrids, decentralized control methods have been proposed for frequency and voltage regulation [160]–[161].

At the inverter level for fast control, BESS usually adopts grid forming control. Most recently, pilot projects of large size BESS relying on grid-forming control have been conducted by GE (30 MW/22 MWh BESS for blackstart, 2017), Hitachi ABB (Dalrymple BESS in South Australia, 30 MW/8 MWh, 2018), and Tesla (Hornsdale BESS in South Australia, two BESS: 100 MW/129 MWh and 150MW/195 MWh) [162]. In those projects, a BESS is able to generate its own voltage and frequency references. It can operate in a microgrid serving as the sole energy source. For example, GE's 30 MW BESS used for black starting large gas turbines has the capabilities of direct start of large asynchronous machines, large transformer energizing [163]. In both cases, large current and reactive power are needed. BESS's voltage can be controlled to gradually increase to achieve soft energizing and reduce inrush current. Similarly, Hitachi ABB's 30 MW BESS, with the capability to black start a local 33 kV distribution network with 8 MW demand, also adopts a soft energizing method [164].

B. Electricity Market Regulations on Energy Storage

Wholesale market rules were established around legacy assets. These rules restrict the full potential of modern storage sources. Thus, different countries have started to revise and upgrade their market regulations to facilitate the participation of ESSs in energy and ancillary markets.

In the U.S., as an example, the FERC Order 755 lays out the regulation requirements of new pay-for-performance markets for frequency regulation services. The regulation intends to reward the fast and accurate performance of energy storage [165]. In the past, there have been pumped-hydro ESSs providing energy and ancillary services in some RTO/ISO markets. However, these ESSs had to use whatever participation model existed then. Such a model was initially designed to accommodate traditional generation/demand resources and would not treat electric storage resources as they are. Thus, the capabilities of ESSs in providing capacity, energy, and ancillary services to the RTO/ISO markets would be left unrecognized. Later, it was also noted that the RTO/ISO tariffs, which existed then, would limit smaller electric storage resources in participating in the RTO/ISO markets as demand response resources, which would restrict the electric storage resources' ability to employ their full operational range, prohibit them from injecting power into the grid, and would preclude them from providing certain services that they were technically capable of (such as operating reserves) [166].

The aforementioned shortcomings caused the need for a proper regulatory design as a key factor in allowing for the efficient deployment of storage technology to be recognized [167]. The order [166] requires that the participation model must: 1) ensure that a resource using the participation model is eligible to provide all capacity, energy, and ancillary services that the resource is technically capable of providing in the RTO/ISO markets as participating in multiple market opportunities will improve the economic feasibility of storage projects; 2) ensure that a participating storage resource is dispatchable and can set the wholesale market clearing price as both a wholesale seller and wholesale buyer consistent with existing market rules that govern when a resource can set the wholesale price; 3) account for the physical and operational characteristics of electric storage resources through bidding parameters or other means; and 4) establish a minimum size requirement for participation in the RTO/ISO

markets that does not exceed 100 kW [165], [168]. Also, each RTO/ISO must specify that the sale of electric energy from the RTO/ISO markets to an ESS that the ESS then resells back to those markets must be at the wholesale locational marginal price.

The order also redefined an ESS as "a resource capable of receiving electric energy from the grid and storing it for later injection of electricity back to the grid regardless of where the resource is located on the electrical system" to broaden its application [166]. Also, it would not be important whether the resource is located on the bulk grid or on a distribution system. Additionally, it was clarified that even behind-the-meter storage resources fall under this definition [166].

The order also suggested that electric storage resources should be eligible, as a part of the participation model, to provide services that are not procured by the RTOs/ISOs through a market mechanism, such as black-start service, primary frequency regulation reserve, and reactive power service provided they possess the required technical capability to provide the aforesaid services. Furthermore, the order clearly says that separate participation models are not necessary for different kinds of ESSs (e.g., slower, faster, or aggregated) because the technical differences between ESSs may be represented by complying with the requirements for bidding parameters, meaning a single participation model can be designed to be flexible enough to accommodate any type of ESS.

C. Applications in Different Markets

In PJM, batteries used to participate in the regulation market by submitting two-part offers (capability and performance); while in the energy market they could only submit positive MW offers (discharging offers) with a $0 offer price [169]–[171]. However, the PJM market is now redesigned to comply with the FERC Order 841. Batteries are now allowed to submit charging, discharging, and continuous mode operation bids/offers based on their cost curves to participate in the energy market [10]. In New England ISO, under the ongoing market design changes, a battery system sized 5 MW or larger would be able to participate in the regulation market as of December 2019 [10].

The California Independent System Operator (CAISO) has already designed a market model that supports the participation of energy-limited ESSs and considers constraints on their SOC as well as on their maximum charge and discharge capacity [127]. Thereby, in CAISO, batteries can participate in the day-ahead and real-time regulation markets by submitting simple price-quantity based bids/offers. New York Independent System Operator (NYISO) might be the first grid operator to allow BESSs to generate revenue as both wholesale and retail energy resources. It might be the first to make possible the dual participation of batteries, as required by Order 841 [172].

The Federal Network Agency of Germany updated its bidding times and minimum bid size for secondary and tertiary frequency control. In July 2018, Germany adjusted the secondary and tertiary frequency control bidding times from weekly to daily basis. The regulatory adjustments have made possible the participation of BESSs in the ancillary services market. Such a daily bidding also allows the storage capacity to participate in more target markets [173]. However, there still exist a number of technical requirements for a unit participating in the German secondary regulation market that may limit BESSs. From a battery storage perspective, two of these requirements include the capability to reach the offered power within 5 minutes and to continue providing that power for 4 hours [174]. Although the former is not an issue for BESSs, the latter may be limiting.

In July 2017, the United Kingdom's Office of Gas and Electricity Markets and the Department for Business, Energy & Industrial Strategy revealed the "Smart Systems and Flexibility Plan", the UK's most important document for promoting energy storage in the energy market. In compliance with this market change, in May 2018, U.K. transmission operator National Grid released a report, announcing the creation of "Virtual Lead Party", a new category of market participant, as well as "secondary balancing mechanism units (SBMU)", a new balancing market service provider [173].

In Chile, following the presidential order on a long-term national energy strategy that targets generating at least 70% of the electricity from renewable sources by 2050, the national energy commission issued new ancillary services regulations that would pave the way for BESSs to offer rapid frequency response services [175]. In August 2017, the Australian Energy Market Commission (AEMC) released its "National Electricity Amendment Rule 2017" to open up its ancillary services market to new participants other than large power generation companies. The rule has greatly increased the opportunities for ESSs to participate in the ancillary services market. The rule aims to make the competition fair for behind-the-meter resources when participating in the electricity market by clarifying the various services that behind-the-meter resources can offer [173].

Finally, it can be said that research topics such as storage ownership and operation, the necessity to upgrade regulatory mechanisms, degradation cost model of ESSs [10], and bidding strategies [127] are still among the ongoing debates surrounding the participation of ESSs in electricity markets. For further details on applications, market participations, and integration of grid-connected batteries, readers are referred to [14].

V. Global Battery Energy Storage Projects

In this section, a review of global stationary battery energy storage projects is presented. The given statistics are slightly underestimated as decentralized battery storage is not included. The data is obtained from International Energy Agency (IEA) [176] and the U.S. DOE global energy storage database [177]. Fig. 8 shows the geographic distribution of the global battery storage projects and provides a tangible representation of what the status quo is. The data includes announced, contracted, and constructed projects. It can be seen that most of the projects are in the United States, Europe (particularly Germany), Japan, China, South Korea, and Australia.

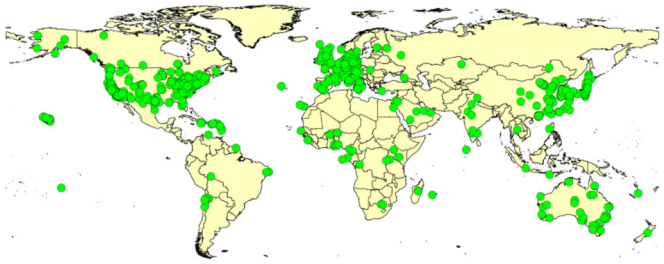

Fig. 8. The geographic distribution of battery energy storage projects [177].

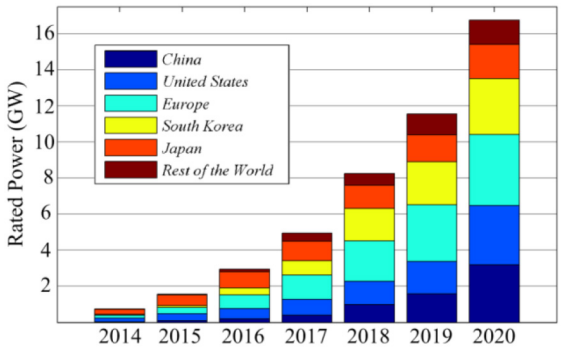

Fig. 9. Cumulative rated power (GW) of battery storage plants deployed worldwide [176].

As Fig. 8 shows, the number of projects in the United States and Germany is quite significant.

Despite the many challenges associated with the supply chain and shipping constraints due to COVID-19, in early 2021, the world's largest BESS (400 MW/1600 MWh) became operational in Monterey County, California and out-scaled the 250 MW/250 MWh Gateway energy storage facility already installed in San Diego. The Monterey BESS is extendable up to 1500 MW/6000 MWh according to Vistra, the company who deployed it. The project is housed inside a gas power plant and comprises more than 4500 stacked battery racks, each of which consists of 22 individual battery modules [178]. The BESS absorbs surplus energy from the grid during daylight hours, which helps slightly mitigate the Duck curve issue in California where electricity generation by PV power plants is abundant. The stored energy is then used to help the network meet its peak demand. Both the Monterey and Gateway storage facilities use Li-ion batteries.

A few BESS-aided Automatic Generation Control (AGC) projects have been practically employed in China. These BESSs are installed within coal-fired power plants in regions with significant renewables. For instance, there is a 2 MW/0.5 MWh BESS deployed at Shijingshan, a major frequency regulation thermal power plant in Beijing City. The BESS works coordinately with the generating unit to improve AGC performance [179].

Tohoku Power Electric, a Japanese power utility, installed 40 MW/20 MWh BESS at Sendai-Nishi substation in 2015 as a part of a demonstration project funded by the Ministry of Economy, Trade, and Industry [180]. The project aims to be an actual demonstration of a frequency regulation control [181] where the BESS compensates short-term fluctuations, and thermal power plants compensate for mid-term and long-term fluctuations. In Oki Islands in Japan, where electricity is mainly produced by renewables and hydropower plants, supply/demand flexibility has been improved using a BESS consisting of Li-ion (2 MW/ 0.7 MWh) and sodium-sulfur batteries (4.2 MW/ 25.2 MWh) [182].

Just two years after a devastating blackout hit the United Kingdom, Europe's largest battery energy storage project (100 MW/100 MWh) at Minety plant in Wiltshire, U.K. is now successfully grid-connected. The system will store the surplus electricity from the UK's national grid when demand is low and renewables are high and then evacuate it back into the grid as demand peaks. The Minety project, which uses $LiFePO_4$ batteries, now outsizes the once-the-largest 48 MW European storage facility which was developed in Jardelund, Germany for primary frequency reserve purposes [183].

The Dalian project in China, which is going to be fully operational soon, is the largest (200 MW/800 MWh) Vanadium Redox Flow (VRF) battery storage system ever intended [184]. It is grid-tied, delivering power to the grid during the peak hours and charging up from the grid during light-load hours. Smaller capacity VRF battery projects are also in operation in other countries, including the 15 MW/60 MWh Minami Hayakita Substation in Japan [185].

Fig. 9 shows the development of battery storage systems in terms of cumulative rated power since 2014. As the figure shows, the total installed battery storage capacity reached nearly 17 GW as of the end of 2020. As seen, the United States and China together led around 3 GW out of the total 5 GW storage capacity added in 2020.

The statistics recently revealed by Wood Mackenzie Power & Renewables [186] predict that the annual U.S. energy storage deployments will reach nearly 7 GW in 2025. The report says that even taking into account the impacts of COVID-19, the U.S. energy storage market will cross the threshold of $6.9 billion by 2025.

In addition to the aforesaid stationary storage projects, there also are a few Transportable Energy Storage Systems (TESSs) recently deployed throughout the world. For example, in the U.S., electric utility company Premium Power's 0.5 MW/2.8 MWh transportable Zinc-Bromine energy storage system was set up by the Electric Power Research Institute (EPRI) [187]. Li-ion manufacturer Altair Nanotechnologies now has 1 MW/250 kWh trailer-mounted Li-ion battery systems in service with both AES Corporation and PJM interconnection [187]. Having added 30 new 338 kWh mobile battery energy storage systems from Alfen, Greener project in Europe is now scaled up to 15 MWh, the world's largest emission-free mobile power provider [135]. In 2018, SPECO unveiled a new vehicular energy storage system in China [136]. The system is capable of providing services such as load shifting, emergency power supply, backup power, smart charging, and mobile rescue services.

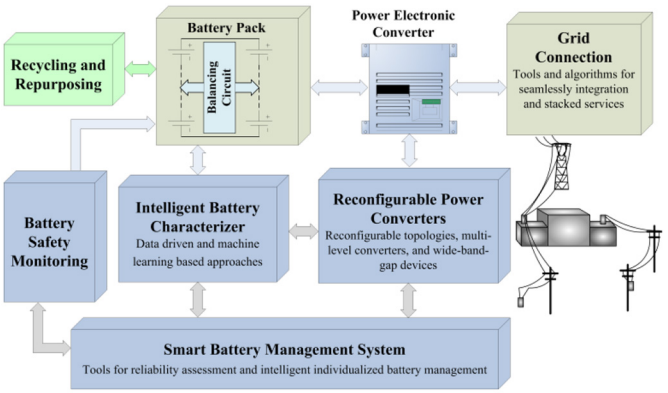

Fig. 10. Tools for reliability assessment, intelligent individualized battery management, and safety monitoring.

VI. Challenges in Implementing and Managing Grid-Connected BESSs

Although there has been phenomenal growth of BESS worldwide, a wide range of challenges still need to be addressed to achieve sustainable development and wide deployment of BESSs in power systems. Holistic and updated analysis of the relationship between the characterization, modeling, management, and applications of grid-tied BESSs will remain to be a grand challenge as battery storage is a dynamic research area. Nevertheless, in this section, the focus is given to the challenges in battery management, reliability analysis, and energy management of grid-connected BESSs, shown in Fig. 10. The research challenges related to battery safety, battery material recycling, and second-life applications of used batteries are briefly discussed as well.

A. Smart BMS

An effective BMS is essential to any battery systems, particularly grid-connected BESSs. Accurate SOC and SOH estimation remains one of the fundamental challenges for a BMS. As more real operating data of different battery systems under different operating conditions have been collected, data driven and machine learning approaches will become a main trend for SOC and SOH estimation [102], [135]. Another development trend is to develop new sensors that can be embedded inside battery cells for SOC (and/or SOH) estimation from the perspective of hardware advancement [20].

In addition to the improvements and breakthroughs needed from material science on batteries, it is equally important to develop advanced BMS for reliability enhancement via new power electronic converters. Most current battery systems are interconnected in a fixed manner, and a single failure of a battery can result in severe damage and the failure of the whole system. As such, reconfigurable battery systems have been previously proposed to handle battery failures [133]. However, in the existing approaches, another layer of circuit has been added to achieve the function of reconfiguration, which increases the cost and reduces the efficiency. It is thus necessary to develop a smart power electronic converter to achieve individualized management for reliability and durability enhancement of large-scale BESSs. The recent advancement in wide bandgap (WBG) devices such as SiC and GaN brings new opportunities for the development of multi-level power converters for transformerless grid connected BESSs.

B. Reliability Analysis of Grid-Connected BESS

Reliability has been a great concern for battery systems as there have been several high-profile battery failure events, from small smartphone batteries to medium-size battery packs used in airplanes and EVs. The issue will become much more challenging, and the results could be much worse and catastrophic when we are dealing with large-scale battery systems consisting of hundreds and thousands of battery cells/modules [188]–[189]. Well-established reliability models and analysis methods have been proposed for conventional power system components such as generators, transmission lines, transformers, etc. [190]. It is necessary to also have reliability models of large-scale BESSs and analysis tools for planning and operating of power systems with grid-connected BESSs. Although the traditional reliability assessment method is simple, when it comes to a battery module with thousands of battery cells, the result obtained can be very conservative [131]. The connection of reliability indicators with battery degradation model is yet to be cleared out. Thus, a new health-condition-based reliability evaluation method that can handle variations in battery cells/modules and even heterogeneous batteries as well as partial operating states is of great importance and a great need for large-scale battery systems.

C. Energy Management Tools for Power Systems With Grid-Connected BESSs

As previously discussed, the cost function of a BESS is not as readily available as the generation cost curve of conventional generators. A comprehensive battery cost model is needed to capture various factors including the investment cost, operation and maintenance cost, and degradation cost that depend on how the BESS is being operated. BESSs are capable of following both Regulation A (RegA) and Regulation D (RegD) signals and providing stacked services, i.e., multiple simultaneous grid services, such as voltage support and spinning reserve. Algorithms are needed to seamlessly integrate BESS dispatch models with the existing energy management systems for long-term planning and real-time operation. Tools and algorithms are also needed to dynamically allocate the capacity of a BESS to achieve simultaneous stacked services.

D. Battery Safety

The issue of safety will continue to be an essential factor that significantly affects the growth of the Li-ion battery industry, as reflected in recent research attempts on battery fire causes [191], suppression medium [192], and protection technologies [193]. However, less attention has been given to battery fire detection instrumentation. Thus, on one hand, it is imperative to perform research to enhance grid resilience by promoting a safer design of battery storage facilities; on

the other hand, it is critical to devise innovative instruments for battery fire mitigation. Therefore, enhanced fire suppression technologies and fire diagnostic simulators/instruments for Li-ion batteries will be among future research directions. Such instruments need to encompass an acquisition unit with embedded sensors for the real-time collection of battery fire data (e.g., thermal conditions, current flow, impedance, and gas emissions). The data could then be processed using machine learning techniques to identify the features that elucidate the characteristics that help proactively diagnose a battery fire. As of now, there is no way of predicting a battery pack fire at the onset. This is mostly because our knowledge of thermal runaway pertains to the cell level, which is hard to extend to fires in a large battery pack.

E. Battery Recycling and Repurposing of Used Batteries

Mountains of accumulated waste would be the legacy of Li-ion batteries if not produced and used on a well-regulated and sustainable basis, as evidenced by ongoing research efforts [194] as well as the DOE's current call [195] for research proposal on the matter. Improper production and disposal of batteries will remain to be an ever-growing challenge to our environment and health unless the remedial measures are taken now. Current battery recycling facilities are limited and the new materials being used in emerging battery technologies not only complicates the recovery but also restricts the applicability of the recycled materials in other fields. Thus, three of the research directions that could be pursued to mitigate the battery waste issue are: 1) Revisiting battery manufacturing, configuration, and assembly in a way that eases later battery recycling and reuse, 2) Creating advanced facilities for end-of-life battery collection and recycling (e.g., the mining and extraction of lithium, cobalt, nickel, and other scarce metals used in batteries), and 3) Second-life applications for batteries that have been already used to power up EVs [196], such as in stationary [197] or transportable [187] storage units for providing grid services.

VII. Conclusion

Battery energy storage is becoming an important asset to the power grid by providing a wide range of grid supports and services such as supply-demand balancing, fast responsive frequency regulation, power quality, peak shaving and load shifting, reliability enhancement, and system restoration. However, these benefits are contingent upon the battery's efficient operation achieved through proper circuits and algorithms all integrated into a battery management system. In this paper, with a focus on Li-ion batteries, the current state of battery modeling, management, and applications have been extensively reviewed and discussed. As this literature survey shows, further research on battery storage is still required towards "smart batteries for smart power grids". These research interests include, but not limited to, smart battery management with data-driven SOC/SOH estimation, reliability analysis of large scale battery storage systems, and models, algorithms, and tools for energy management of grid-connected battery storage systems.

Acknowledgment

This paper is the work of the Working Group on Management of Distributed Battery Storage Systems, Distributed Energy Resources Subcommittee, EDPG Committee, Power and Energy Society, IEEE.

References

[1] H. Rahimi-Eichi, U. Ojha, F. Baronti, and M. Chow, "Battery management system: An overview of its application in the smart grid and electric vehicles," *IEEE Ind. Electron. Mag.*, vol. 7, no. 2, pp. 4–16, Jun. 2013.

[2] K. Halicka, P. A. Lombardi, and Z. Styczyński, "Future-oriented analysis of battery technologies," in *Proc. IEEE Int. Conf. Ind. Technol. (ICIT)*, 2015, pp. 1019–1024.

[3] N. B. Arias, J. C. López, S. Hashemi, J. F. Franco, and M. J. Rider, "Multi-objective sizing of battery energy storage systems for stackable grid applications," *IEEE Trans. Smart Grid*, vol. 12, no. 3, pp. 2708–2721, May 2021.

[4] T. M. Gür, "Review of electrical energy storage technologies, materials and systems: Challenges and prospects for large-scale grid storage," *Energy Environ. Sci.*, vol. 11, pp. 2696–2767, Jul. 2018.

[5] M. S. Whittingham, "History, evolution, and future status of energy storage," *Proc. IEEE*, vol. 100, pp. 1518–1534, May 2012.

[6] (BloombergNEF, London, U.K.) *Energy Storage Investments Boom As Battery Costs Halve in the Next Decade*. (Jul. 2019). [Online]. Available: https://about.bnef.com/blog/energy-storage-investments-boom-battery-costs-halve-next-decade/

[7] S. M. Samara, M. F. Shaaban, and A. Osman, "Management of mobile energy generation and storage system," in *Proc. IEEE PES GTD Grand Int. Conf. Exposit. Asia (GTD Asia)*, Bangkok, Thailand, 2019, pp. 450–454.

[8] A. Adrees, H. Andami, and J. V. Milanovic, "Comparison of dynamic models of battery energy storage for frequency regulation in power system," in *Proc. 18th Mediterr. Electrotechn. Conf. (MELECON)*, 2016, pp. 1–9, doi: 10.1109/MELCON.2016.7495314.

[9] M. Faisal, M. A. Hannan, P. J. Ker, A. Hussain, M. B. Mansor, and F. Blaabjerg, "Review of energy storage system technologies in microgrid applications: Issues and challenges," *IEEE Access*, vol. 6, pp. 35143–35164, 2018.

[10] A. R. Sparacino, G. F. Reed, R. J. Kerestes, B. M. Grainger, and Z. T. Smith, "Survey of battery energy storage systems and modeling techniques," in *Proc. IEEE Power Energy Soc. Gen. Meeting*, San Diego, CA, USA, 2012, pp. 1–8.

[11] D. N. T. How, M. A. Hannan, M. S. H. Lipu, and P. J. Ker, "State of charge estimation for lithium-ion batteries using model-based and data-driven methods: A review," *IEEE Access*, vol. 7, pp. 136116–136136, 2019.

[12] J. P. Rivera-Barrera, N. Muñoz-Galeano, and H. O. Sarmiento-Maldonado, "SoC estimation for lithium-ion batteries: Review and future challenges," *Electronics*, vol. 6, no. 4, p. 102, 2017.

[13] G. Wang *et al.*, "A review of power electronics for grid connection of utility-scale battery energy storage systems," *IEEE Trans. Sustain. Energy*, vol. 7, no. 4, pp. 1778–1790, Oct. 2016.

[14] M. Stecca, L. R. Elizondo, T. B. Soeiro, P. Bauer, and P. Palensky, "A comprehensive review of the integration of battery energy storage systems into distribution networks," *IEEE J. Ind. Electron. Soc.*, vol. 1, pp. 46–65, 2020.

[15] S. A. Hasib *et al.*, "A comprehensive review of available battery datasets, RUL prediction approaches, and advanced battery management," *IEEE Access*, vol. 9, pp. 86166–86193, 2021.

[16] X. Li and S. Wang, "A review on energy management and operational control methods for grid battery energy storage systems" *IEEE CSEE J. Power Energy Syst.*, vol. 7, no. 5, pp. 1026–1040, Sep. 2021.

[17] M. Naguib, P. Kollmeyer, and A. Emadi, "Lithium-ion battery pack robust state of charge estimation, cell inconsistency, and balancing: Review," *IEEE Access*, vol. 9, pp. 50570–50582, 2021.

[18] Z. Wang, G. Feng, D. Zhen, F. Gu, and A. Ball, "A review on online state of charge and state of health estimation for lithium-ion batteries in electric vehicles," *Energy Rep.*, vol. 7, pp. 5141–5164, Nov. 2021.

[19] Z. B. Omariba, L. Zhang, and D. Sun, "Review of battery cell balancing methodologies for optimizing battery pack performance in electric vehicles," *IEEE Access*, vol. 7, pp. 129335–129352, 2019.

[20] X. Hu, F. Feng, K. Liub, L. Zhang, J. Xie, and B. Liu, "State estimation for advanced battery management: Key challenges and future trends," *Renew. Sustain. Energy Rev.*, vol. 114, pp. 1–13, Oct. 2019.

[21] C. Gervillié, A. Boisard, J. Labbé, S. Berthon-Fabry, and K. Guérin, "Tin-based materials: The future of anode materials for lithium ion battery?" in *Proc. Eur. Space Power Conf. (ESPC)*, Juan-les-Pins, France. Sep. 2019, p. 5, doi: 10.1109/ESPC.2019.8932045.

[22] Y. Mekonnen, A. Sundararajan, and A. I. Sarwat, "A review of cathode and anode materials for lithium-ion batteries," in *Proc. Southeast Conf.*, 2016, pp. 1–6.

[23] A. K. Shukla and T. P. Kumar, "Materials for next generation lithium batteries," *Current Sci.*, vol. 94, no. 3, pp. 317–327, 2008.

[24] X. Chen, W. Shen, T. Vo, Z. Cao, and A. Kapoor, "An overview of lithium-ion batteries for electric vehicles," in *Proc. IPEC Power Energy Conf.*, 2012, pp. 230–235.

[25] B. Diouf and R. Pode, "Potential of lithium-ion batteries in renewable energy," *J. Renew. Energy*, vol. 76, pp. 375–380, Apr. 2015.

[26] A. Bindra, "Electric vehicle batteries eye solid-state technology: Prototypes promise lower cost, faster charging, and greater safety," *IEEE Power Electron. Mag.*, vol. 7, no. 1, pp. 16–19, Mar. 2020.

[27] O. Gross and J. Swoyer, "The next step in low cost lithium-ion polymer systems," in *Proc. IEEE Battery Conf. Appl. Adv.*, 2002, pp. 1–10.

[28] W. Zhuang, S. Lu, and H. Lu, "Progress in materials for lithium-ion power batteries," in *Proc. Int. Conf. Intell. Green Build. Smart Grid (IGBSG)*, 2014, pp. 1–2.

[29] A. Trovò, V. D. Noto, J. E. Mengou, C. Gamabaro, and M. Guarnieri, "Fast response of kW-class vanadium redox flow batteries," *IEEE Trans. Sustain. Energy*, vol. 12, no. 4, pp. 2413–2422, Oct. 2021.

[30] A. Almarzooqi, H. Albeshr, A. Mnatsakanyan, W. Alzahmi, E. Bilbao, and S. Sgouridis, "Optimizing operations of sodium sulfur (NAS) large-scale battery storage," in *Proc. IEEE 11th Int. Symp. Power Electron. Distrib. Gener. Syst. (PEDG)*, 2020, pp. 159–163.

[31] C. Wang, M. H. Nehrir, and S. R. Shaw, "Dynamic models and model validation for PEM fuel cells using electrical circuits," *IEEE Trans. Energy Convers.*, vol. 20, no. 2, pp. 442–451, Jun. 2005.

[32] A. Hentunen, T. Lehmuspelto, and J. Suomela, "Time-domain parameter extraction method for Thévenin-equivalent circuit battery models," *IEEE Trans. Energy Convers.*, vol. 29, no. 3, pp. 558–566, Sep. 2014.

[33] M. T. Lawder, V. Viswanathan, and V. R. Subramanian, "Balancing autonomy and utilization of solar power and battery storage for demand based microgrids," *J. Power Sources*, vol. 279, pp. 645–655, Apr. 2015.

[34] Z. Deng, L. Yang, H. Deng, Y. Cai, and D. Li, "Polynomial approximation pseudo-two-dimensional battery model for online application in embedded battery management system," *Energy*, vol. 142, pp. 838–850, Jan. 2018.

[35] X. Wu, X. Hu, X. Yin, and S. J. Moura, "Stochastic optimal energy management of smart home with PEV energy storage," *IEEE Trans. Smart Grid*, vol. 9, no. 3, pp. 2065–2075, May 2018.

[36] F. Saidani, F. X. Hutter, R.-G. Scurtu, W. Braunwarth, and J. N. Burghartz, "Lithium-ion battery models: A comparative study and a model-based powerline communication," *Adv. Radio Sci.*, vol. 15, pp. 83–91, Apr. 2017.

[37] G. Aurilio *et al.*, "A battery equivalent-circuit model and an advanced technique for parameter estimation," in *Proc. IEEE Int. Instrum. Meas. Technol. Conf. (I2MTC)*, 2015, pp. 1705–1710.

[38] K. Li and K. J. Tseng, "An equivalent circuit model for state of energy estimation of lithium-ion battery," in *Proc. IEEE Appl. Power Electron. Conf. Exposit. (APEC)*, 2016, pp. 3422–3430.

[39] M. D. Murbach and D. T. Schwartz, "Extending Newman's pseudo-two-dimensional lithium-ion battery impedance simulation approach to include the nonlinear harmonic response," *J. Electrochem. Soc.*, vol. 164, no. 11, 2017, Art. no. E3311.

[40] Y. Zou, X. Hu, H. Ma, and S. E. Li, "Combined state of charge and state of health estimation over lithium-ion battery cell cycle lifespan for electric vehicles," *J. Power Sources*, vol. 273, pp. 793–803, Jan. 2015.

[41] X. Hu, L. Johannesson, N. Murgovski, and B. Egardt, "Longevity-conscious dimensioning and power management of the hybrid energy storage system in a fuel cell hybrid electric bus," *Appl. Energy*, vol. 137, pp. 913–924, Jan. 2015.

[42] J. F. Manwell and J. G. McGowan, "Lead acid battery storage model for hybrid energy systems," *Solar Energy*, vol. 50, no. 5, pp. 399–405, 1993.

[43] M. R. Jongerden *et al.*, "Maximizing system lifetime by battery scheduling," in *Proc. 39th Annu. IEEE/IFIP Int. Conf. Depend. Syst. Netw. IEEE Comput. Soc. Press*, 2009, pp. 63–72.

[44] E. I. Vrettos and S. A. Papathanassiou, "Operating policy and optimal sizing of a high penetration RES-BESS system for small isolated grids," *IEEE Trans. Energy Convers.*, vol. 26, no. 3, pp. 744–756, Sep. 2011.

[45] Z. N. Bako, M. A. Tankari, G. Lefebvre, and A. S. Maiga, "Experiment-based methodology of kinetic battery modeling for energy storage," *IEEE Trans. Ind. Appl.*, vol. 55, no. 1, pp. 593–599, Jan./Feb. 2019.

[46] X. Sui, S. He, D. Stroe, X. Huang, J. Meng, and R. Teodorescu, "A review of sliding mode observers based on equivalent circuit model for battery SoC estimation," in *Proc. IEEE 28th Int. Symp. Ind. Electron. (ISIE)*, Vancouver, BC, Canada, 2019, pp. 1965–1970.

[47] A. S. Subburaj, S. B. Bayne, M. G. Giesselmann, and M. A. Harral, "Analysis of equivalent circuit of the utility scale battery for wind integration," *IEEE Trans. Ind. Appl.*, vol. 52, no. 1, pp. 25–33, Jan./Feb. 2016.

[48] M. Bahramipanah, D. Torregrossa, R. Cherkaoui, and M. Paolone, "Enhanced equivalent electrical circuit model of lithium-based batteries accounting for charge redistribution, state-of-health, and temperature effects," *IEEE Trans. Transp. Electrif.*, vol. 3, no. 3, pp. 589–599, Sep. 2017.

[49] V. Sangwan, R. Kumar, and A. K. Rathore, "Estimation of battery parameters of the equivalent circuit model using Grey Wolf optimization," in *Proc. IEEE 6th Int. Conf. Power Syst. (ICPS)*, 2016, pp. 1–6.

[50] B. Chen, H. Ma, H. Fang, H. Fan, K. Luo, and B. Fan, "An approach for state of charge estimation of Li-ion battery based on Thevenin equivalent circuit model," in *Proc. Prognos. Syst. Health Manag. Conf. (PHM-Hunan)*, 2014, pp. 647–652.

[51] C. Unterrieder, R. Priewasser, M. Agostinelli, S. Marsili, and M. Huemer, "Comparative study and improvement of battery open-circuit voltage estimation methods," in *Proc. IEEE 55th Int. Midwest Symp. Circuits Syst. (MWSCAS)*, Boise, ID, USA, 2012, pp. 1076–1079.

[52] T. Wada, T. Takegami, and Y. Wang, "Sequential estimation of state of charge and equivalent circuit parameters for lithium-ion batteries," in *Proc. Amer. Control Conf. (ACC)*, Chicago, IL, USA, 2015, pp. 2494–2498.

[53] M. Chen, and G. A. Rincon-Mora, "Accurate electrical battery model capable of predicting runtime and I–V performance," *IEEE Trans. Energy Convers.*, vol. 21, no. 2, pp. 504–511, Jun. 2006.

[54] C. Duan, C. Wang, and M. Liu, "A fast approach for predicting battery open circuit voltage based on exponential recovery voltage," in *Proc. North Amer. Power Symp. (NAPS)*, Morgantown, WV, USA, 2017, pp. 1–5.

[55] M. Farag, M. Fleckenstein, and S. Habibi, *Li-Ion Battery SOC Estimation Using Non-Linear Estimation Strategies Based on Equivalent Circuit Models*, SAE, Warrendale, PA, USA, 2014.

[56] M. Hossain, S. Saha, M. E. Haque, M. T. Arif, and A. Oo, "A parameter extraction method for the thevenin equivalent circuit model of Li-ion batteries," in *Proc. IEEE Ind. Appl. Soc. Annu. Meeting*, Baltimore, MD, USA, 2019, pp. 1–7.

[57] G. Liu *et al.*, "A comparative study of equivalent circuit models and enhanced equivalent circuit models of lithium-ion batteries with different model structures," in *Proc. IEEE Conf. Expo Transp. Electrif. Asia–Pac. (ITEC Asia–Pacific)*, Beijing, China, 2014, pp. 1–6.

[58] C. Zou, L. Zhang, X. Hu, Z. Wang, T. Wik, and M. Pecht, "A review of fractional-order techniques applied to lithium-ion batteries, lead-acid batteries, and supercapacitors," *J. Power Sources*, vol. 390, pp. 286–296, Jun. 2018.

[59] C. Zou, X. Hu, S. Dey, L. Zhang, and X. Tang, "Nonlinear fractional-order estimator with guaranteed robustness and stability for lithium-ion batteries," *IEEE Trans. Ind. Electron.*, vol. 65, no. 7, pp. 5951–5961, Jul. 2018.

[60] X. Hu, H. Yuan, C. Zou, Z. Li, and L. Zhang, "Co-estimation of state of charge and state of health for lithium-ion batteries based on fractional-order calculus," *IEEE Trans. Veh. Technol.*, vol. 67, no. 11, pp. 10319–10329, Nov. 2018.

[61] A. Ahsan, Q. Zhao, A. M. Khambadkone, and M. H. Chia, "Dynamic battery operational cost modeling for energy dispatch," in *Proc. IEEE Energy Convers. Congr. Exposit. (ECCE)*, Milwaukee, WI, USA, 2016, pp. 1–5.

[62] B. Asghari, A. Hooshmand, and R. Sharma, "An Amp-hour based electricity cost model for economic dispatch of batteries in microgrids," in *Proc. IEEE PES T&D Conf. Exposit.*, Chicago, IL, USA, 2014, pp. 1–5.

[63] C. Goebel, H. Hesse, M. Schimpe, A. Jossen, and H. Jacobsen, "Model-based dispatch strategies for lithium-ion battery energy storage applied to pay-as-bid markets for secondary reserve," *IEEE Trans. Power Syst.*, vol. 32, no. 4, pp. 2724–2734, Jul. 2017.

[64] M. M. Baggu, A. Nagarajan, D. Cutler, D. Olis, T. O. Bialek, and M. Symko-Davies, "Coordinated optimization of multiservice dispatch for energy storage systems with degradation model for utility applications," *IEEE Trans. Sustain. Energy*, vol. 10, no. 2, pp. 886–894, Apr. 2019.

[65] W. Tang and R. Jain, "Dynamic economic dispatch game: The value of storage," *IEEE Trans. Smart Grid*, vol. 7, no. 5, pp. 2350–2358, Sep. 2016.

[66] T. Das, V. Krishnan, and J. D. McCalley, "High-fidelity dispatch model of storage technologies for production costing studies," *IEEE Trans. Sustain. Energy*, vol. 5, no. 4, pp. 1242–1252, Oct. 2014.

[67] Z. Zhang, J. Wang, T. Ding, and X. Wang, "A two-layer model for microgrid real-time dispatch based on energy storage system charging/discharging hidden costs," *IEEE Trans. Sustain. Energy*, vol. 8, no. 1, pp. 33–42, Jan. 2017.

[68] M. Koller, T. Borsche, A. Ulbig, and G. Andersson, "Defining a degradation cost function for optimal control of a battery energy storage system," in *Proc. IEEE Grenoble Conf.*, 2013, pp. 1–6.

[69] M. Seydenschwanz, K. Majewski, C. Gottschalk, and R. Fink, "Linear approximation of cyclic battery aging costs for MILP-based power dispatch optimization," in *Proc. IEEE PES Innov. Smart Grid Technol. Europe (ISGT-Europe)*, 2019, pp. 1–5.

[70] W. Chen, J. Qiu, J. Zhao, Q. Chai, and Z. Y. Dong, "Bargaining game-based profit allocation of virtual power plant in frequency regulation market considering battery cycle life," *IEEE Trans. Smart Grid*, vol. 12, no. 4, pp. 2913–2928, Jul. 2021.

[71] P. Yong *et al.*, "Evaluating the dispatchable capacity of base station backup batteries in distribution networks," *IEEE Trans. Smart Grid*, vol. 12, no. 5, pp. 3966–3979, Sep. 2021.

[72] N. Y, Soltani and A. Nasiri, "Chance-constrained optimization of energy storage capacity for microgrids," *IEEE Trans. Smart Grid*, vol. 11, no. 4, pp. 2760–2770, Jul. 2020.

[73] Q. Ouyang, J. Chen, J. Zheng, and H. Fang, "Optimal cell-to-cell balancing topology design for serially connected lithium-ion battery packs," *IEEE Trans. Sustain. Energy*, vol. 9, no. 1, pp. 350–360, Jan. 2018.

[74] M. Koseoglou, E. Tsioumas, N. Jabbour, and C. Mademlis, "Highly effective cell equalization in a lithium-ion battery management system," *IEEE Trans. Power Electron.*, vol. 35, no. 2, pp. 2088–2099, Feb. 2020.

[75] B. Dong, Y. Li, and Y. Han, "Parallel architecture for battery charge equalization," *IEEE Trans. Power Electron.*, vol. 30, no. 9, pp. 4906–4913, Sep. 2015.

[76] T. Kim, W. Qiao, and L. Qu, "A series-connected self-reconfigurable multicell battery capable of safe and effective charging/discharging and balancing operations," in *Proc. 27th Annu. IEEE Appl. Power Electron. Conf. Expo.*, 2012, pp. 2259–2264.

[77] M.-Y. Kim, C.-H. Kim, J.-H. Kim, and G.-W. Moon, "A chain structure of switched capacitor for improved cell balancing speed of lithium-ion batteries," *IEEE Trans. Ind. Electron.*, vol. 61, no. 8, pp. 3989–3999, Aug. 2014.

[78] X. Lu, W. Qian, and F. Z. Peng, "Modularized buck-boost + Cuk converter for high voltage series connected battery cells," in *Proc. 27th Annu. IEEE Appl. Power Electron. Conf. Expo.*, 2012, pp. 2272–2278.

[79] M.-Y. Kim, J.-H. Kim, and G.-W. Moon, "Center-cell concentration structure of a cell-to-cell balancing circuit with a reduced number of switches," *IEEE Trans. Power Electron.*, vol. 29, no. 10, pp. 5285–5297, Oct. 2014.

[80] C. Duan, H. Tao, C. Wang, J. Chen, X. Zhao, and X. Zhou, "An electric vehicle battery modular balancing system based on solar energy harvesting," in *Proc. IEEE Transp. Electrif. Conf. Expo (ITEC)*, Detroit, MI, USA, 2019, pp. 1–7.

[81] E. Chatzinikolaou and D. J. Rogers, "A comparison of grid-connected battery energy storage system designs," *IEEE Trans. Power Electron.*, vol. 32, no. 9, pp. 6913–6923, Sep. 2017.

[82] X. Huang, X. Sui, D. Stroe, and R. Teodorescu, "A review of management architectures and balancing strategies in smart batteries," in *Proc. 45th Annu. Conf. IEEE Ind. Electron. Soc. (IECON)*, Lisbon, Portugal, 2019, pp. 5909–5914.

[83] E. B. Haghighi and M. Moghaddam, "Analyzing thermal management methods of Li-ion battery modules," in *Proc. IEEE Int. Telecommun. Energy Conf. (INTELEC)*, 2018, pp. 1–4.

[84] P. Goli and A. A. Balandin, "Graphene-enhanced phase change materials for thermal management of battery packs," in *Proc. 14th Intersoc. Conf. Thermal Thermomechan. Phenom. Electron. Syst. (ITherm)*, Orlando, FL, USA, 2014, pp. 1390–1393.

[85] *IEEE/ASHRAE Draft Guide for the Ventilation and Thermal Management of Batteries for Stationary Applications*, IEEE Standard P1635/ASHRAE 21/D13, Dec. 2017.

[86] Z. Liu, H. X. Li, and H. X. Li, "Thermal modeling for vehicle battery system: A brief review," in *Proc. Int. Conf. Syst. Sci. Eng. (ICSSE)*, Dalian, Liaoning, China, 2012, pp. 74–78.

[87] F. Altaf, B. Egardt, and L. J. Mårdh, "Load management of modular battery using model predictive control: Thermal and state-of-charge balancing," *IEEE Trans. Control Syst. Technol.*, vol. 25, no. 1, pp. 47–62, Jan. 2017.

[88] S. Al-Hallaj, R. Kizilel, A. Lateef, R. Sabbah, M. Farid, and J. R. Selman, "Passive thermal management using phase change material (PCM) for EV and HEV Li-ion batteries," in *Proc. IEEE Veh. Power Propulsion Conf.*, Chicago, IL, USA, 2005, pp. 1–5.

[89] J. Zhang, L. Zhang, F. Sun, and Z. Wang, "An overview on thermal safety issues of lithium-ion batteries for electric vehicle application," *IEEE Access*, vol. 6, pp. 23848–23863, 2018.

[90] Z. Liu and H. Li, "Integrated modeling for intelligent battery thermal management," in *Proc. IEEE Int. Conf. Syst. Man Cybern.*, 2013, pp. 2522–2527.

[91] S. S. Madani, M. J. Swierczynski, and S. K. Kær, "A review of thermal management and safety for lithium ion batteries," in *Proc. 12th Int. Conf. Ecol. Veh. Renew. Energies (EVER)*, 2017, pp. 1–20.

[92] F. Altaf, L. Johannesson, and B. Egardt, "Simultaneous thermal and state-of-charge balancing of batteries: A review," in *Proc. IEEE Veh. Power Propulsion Conf. (VPPC)*, 2014, pp. 1–7.

[93] D. C. Erb, I. M. Ehrenberg, S. E. Sarma, and E. Carlson, "Effects of cell geometry on thermal management in air-cooled battery packs," in *Proc. IEEE Transp. Electrif. Conf. Expo (ITEC)*, Dearborn, MI, USA, 2015, pp. 1–6.

[94] K. S. Ng, C.-S. Moo, Y.-P. Chen, and Y.-C. Hsieh, "Enhanced coulomb counting method for estimating state-of-charge and state-of-health of lithium-ion batteries," *Appl. Energy*, vol. 86, no. 9, pp. 1506–1511, 2009.

[95] U. Datta, A. Kalam, and J. Shi, "Battery energy storage system control for mitigating PV penetration impact on primary frequency control and state-of-charge recovery," *IEEE Trans. Sustain. Energy*, vol. 11, no. 2, pp. 746–757, Apr. 2020.

[96] K. Huang, Y. F. Guo, and Z. G. Li, "Overview of state-of-charge estimation for power lithium-ion batteries," *Power Technol.*, vol. 42, pp. 1398–1401, May 2019.

[97] H. Rahimi-Eichi, F. Baronti, and M. Y. Chow, "Modeling and online parameter identification of Li-polymer battery cells for SOC estimation," in *Proc. IEEE Int. Symp. Ind. Electron. (ISIE)*, 2012, pp. 1336–1341.

[98] L. Liu, L. Y. Wang, Z. Chen, C. Wang, F. Lin, and H. Wang, "Integrated system identification and state-of-charge estimation of battery systems," *IEEE Trans. Energy Convers.*, vol. 28, no. 1, pp. 12–23, Mar. 2013.

[99] Z. He, Y. Liu, M. Gao, and C. Wang, "A joint model and SOC estimation method for lithium battery based on the sigma point KF," in *Proc. IEEE Transp. Electrif. Conf. Expo (ITEC)*, Dearborn, MI, USA, 2012, pp. 1–5.

[100] H. Beelen, H. J. Bergveld, and M. C. F. Donkers, "Joint estimation of battery parameters and state of charge using an extended Kalman filter: A single-parameter tuning approach," *IEEE Trans. Control Syst. Technol.*, vol. 29, no. 3, pp. 1087–1101, May 2021, doi: 10.1109/TCST.2020.2992523.

[101] M. A. Hannan, M. S. H. Lipu, A. Hussain, and A. Mohamed, "A review of lithium-ion battery state of charge estimation and management system in electric vehicle applications: Challenges and recommendations," *Renew. Sustain. Energy Rev.*, vol. 78, pp. 834–854, Oct. 2017.

[102] W. Zhou, Y. Zheng, Z. Pan, and Q. Lu, "Review on the battery model and SOC estimation method," *Processes*, vol. 9, no. 9, pp. 1–23, 2021.

[103] B. Xia, C. Chen, Y. Tian, W. Sun, Z. Xu, and W. Zheng, "A novel method for state of charge estimation of lithium-ion batteries using a nonlinear observer," *J. Power Sources*, vol. 270, pp. 359–366, Dec. 2014.

[104] L. Wang, S. L. Wang, and L. Chen, "An improved estimation method of lithium battery SoC particle filter," *Battery Ind.*, vol. 22, no. 2, pp. 120–123, 2018.

[105] B. Xiong, J. Zhao, Y. Su, Z. Wei, and M. Skyllas-Kazacos, "State of charge estimation of vanadium redox flow battery based on sliding mode observer and dynamic model including capacity fading factor," *IEEE Trans. Sustain. Energy*, vol. 8, no. 4, pp. 1658–1667, Oct. 2017.

[106] X. Sui, Y. C. Chen, and X. H. Zhang, "Method of estimating state of charge of Li-ion battery based on improved sliding mode observer," *New Electr. Energy Technol.*, vol. 37, no. 11, pp. 73–82, 2018.

[107] X. Chen, W. Shen, Z. Cao, and A. Kapoor, "A novel approach for state of charge estimation based on adaptive switching gain sliding mode observer in electric vehicles, *J. Power Sources*, vol. 246, pp. 667–678, Jan. 2014.

[108] M. Lagraoui, S. Doubabi, and A. Rachid, "SOC estimation of Lithium-ion battery using Kalman filter and Luenberger observer: A comparative study," in *Proc. Int. Renew. Sustain. Energy Conf. (IRSEC)*, 2014, pp. 636–641.

[109] J. Tian, R. Xiong, W. Shen, and J. Lu, "State-of-charge estimation of LiFePO4 batteries in electric vehicles: A deep-learning enabled approach," *Appl. Energy*, vol. 291, pp. 1–10, Jun. 2021.

[110] S. Tong, J. H. Lacap, and J. W. Park, "Battery state of charge estimation using a load-classifying neural network," *Energy Storage*, vol. 7, pp. 236–243, Aug. 2016.

[111] W. He, N. Williard, C. Chen, and M. Pecht, "State of charge estimation for Li-ion batteries using neural network modeling and unscented Kalman filter-based error cancellation," *Int. J. Electr. Power Energy Syst.*, vol. 62, pp. 783–791, Nov. 2014.

[112] P. Singh, R. Vinjamuri, X. Wang, and D. Reisner, "Design and implementation of a fuzzy logic-based state-of-charge meter for Li-ion batteries used in portable defibrillators," *J. Power Sources*, vol. 162, no. 2, pp. 829–836, 2006.

[113] I. Li, W. Wang, S. Su, and Y. Lee, "A merged fuzzy neural network and its applications in battery state-of-charge estimation," *IEEE Trans. Energy Convers.*, vol. 22, no. 3, pp. 697–708, Sep. 2007.

[114] X. T. Liu, K. Li, and J. Wu, "Power battery SoC estimation based on EKF-SVM algorithm," *Autom. Eng.*, vol. 42, pp. 1522–1528, Oct. 2020.

[115] X. Wu, L. Mi, W. Tan, J. L. Qin, and M. N. Zhao, "State of charge (SoC) estimation of Ni-MH battery based on least square support vector machines," *Adv. Mater. Res.*, vols. 211–212, pp. 1204–1209, Feb. 2011.

[116] C. Kunlong, J. Jiuchun, Z. Fangdan, S. Bingxiang, and Z. Yanru, "SOH estimation for Lithium-ion batteries: A cointegration and error correction approach," in *Proc. IEEE Int. Conf. Progn. Health Manag. (ICPHM)*, Ottawa, ON, Canada, 2016, pp. 1–6.

[117] B. Balagopal and M. Chow, "The state of the art approaches to estimate the state of health (SOH) and state of function (SOF) of lithium Ion batteries," in *Proc. IEEE 13th Int. Conf. Ind. Informat. (INDIN)*, Cambridge, U.K., 2015, pp. 1302–1307.

[118] C. Lyu, Y. Zhao, W. Luo, and L. Wang, "Aging mechanism analysis and its impact on capacity loss of lithium ion batteries," in *Proc. 14th IEEE Conf. Ind. Electron. Appl. (ICIEA)*, 2019, pp. 2148–2153.

[119] P. Kubiak, Z. Cena, C. M. López, and I. Belharouak, "Calendar aging of a 250 kW/500 kWh Li-ion battery deployed for the grid storage application," *J. Power Sources*, vol. 372, pp. 16–23, Dec. 2017.

[120] K. Smith, A. Saxon, M. Keyser, B. Lundstrom, Z. Cao, and A. Roc, "Life prediction model for grid-connected Li-ion battery energy storage system," in *Proc. Amer. Control Conf. (ACC)*, 2017, pp. 4062–4068.

[121] J. Kraenzl, T. T. Nguyen, and A. Jossen, "Investigating stationary storage applications and their impact on battery aging," in *Proc. 14th Int. Conf. Ecol. Veh. Renew. Energies (EVER)*, 2019, pp. 1–9.

[122] D. Werner, S. Paarmann, and T. Wetzel, "Calendar aging of Li-ion cells—Experimental investigation and empirical correlation," *Batteries*, vol. 7, no. 28, pp. 1–23, 2021.

[123] D. Stroe, M. Swierczynski, S. K. Kaer, and R. Teodorescu, "Degradation behavior of lithium-ion batteries during calendar ageing—The case of the internal resistance increase," *IEEE Trans. Ind. Appl.*, vol. 54, no. 1, pp. 517–525, Jan./Feb. 2018.

[124] K. Liu, T. R. Ashwin, X. Hu, M. Lucu, and W. D. Widanage, "An evaluation study of different modelling techniques for calendar ageing prediction of lithium-ion batteries," *Renew. Sustain. Energy Rev.*, vol. 131, pp. 1–14, Oct. 2020.

[125] M. Petricca, D. Shin, A. Bocca, A. Macii, E. Macii, and M. Poncino, "Automated generation of battery aging models from datasheets," in *Proc. IEEE 32nd Int. Conf. Comput. Design (ICCD)*, 2014, pp. 483–488.

[126] F. Chang, F. Roemer, and M. Lienkamp, "Influence of current ripples in cascaded multilevel topologies on the aging of lithium batteries," *IEEE Trans. Power Electron.*, vol. 35, no. 11, pp. 11879–11890, Nov. 2020.

[127] B. Xu, J. Zhao, T. Zheng, E. Litvinov, and D. S. Kirschen, "Factoring the cycle aging cost of batteries participating in electricity markets," *IEEE Trans. Power Syst.*, vol. 33, no. 2, pp. 2248–2259, Mar. 2018.

[128] B. Xu, Y. Shi, D. S. Kirschen, and B. Zhang, "Optimal battery participation in frequency regulation markets," *IEEE Trans. Power Syst.*, vol. 33, no. 6, pp. 6715–6725, Nov. 2018.

[129] Q. Yu, R. Xiong, C. Lin, W. Shen, and J. Deng, "Lithium-ion battery parameters and state-of-charge joint estimation based on *H*-infinity and unscented Kalman filters," *IEEE Trans. Veh. Technol.*, vol. 66, no. 10, pp. 8693–8701, Oct. 2017.

[130] D. Andre, C. Appel, T. Soczka-Guth, and D. U. Sauer, "Advanced mathematical methods of SOC and SOH estimation for lithium-ion batteries," *J. Power Sources*, vol. 224, pp. 20–27, Feb. 2013.

[131] M. Liu, W. Li, C. Wang, M. P. Polis, L. Y. Wang, and J. Li, "Reliability evaluation of large scale battery energy storage systems," *IEEE Trans. Smart Grid*, vol. 8, no. 6, pp. 2733–2743, Nov. 2017.

[132] J. Wang *et al.*, "Cycle-life model for graphite-LiFePO4 cells," *J. Power Sources*, vol. 196, no. 8, pp. 3942–3948, 2011.

[133] L. He, Z. Yang, Y. Gu, C. Liu, T. He, and K. G. Shin, "SoH-aware reconfiguration in battery packs," *IEEE Trans. Smart Grid*, vol. 9, no. 4, pp. 3727–3735, Jul. 2018.

[134] X. Hu *et al.*, "Battery lifetime prognostics," *Joule*, vol. 4, no. 2, pp. 310–346, 2020.

[135] S. Khaleghi, Y. Firouz, J. V. Mierlo, and P. V. D. Bossche, "Developing a real-time data-driven battery health diagnosis method, using time and frequency domain condition indicators," *Appl. Energy*, vol. 255, pp. 1–13, Dec. 2019.

[136] S. Zhang, B. Zhai, X. Guo, K. Wang, N. Peng, and X. Zhang, "Synchronous estimation of state of health and remaining useful lifetime for Lithium ion battery using the incremental capacity and artificial neural networks," *Energy Storage*, vol. 26, Dec. 2019, Art. no. 100951.

[137] M. S. H. Lipu *et al.*, "A review of state of health and remaining useful life estimation methods for lithium-ion battery in electric vehicles: Challenges and recommendations," *J. Clean. Prod.*, vol. 205, pp. 115–133, Dec. 2018.

[138] A. Zenati, P. Desprez, H. Razik, and S. Rael, "Impedance measurements combined with the fuzzy logic methodology to assess the SOC and SOH of lithium-ion cells," in *Proc. IEEE Veh. Power Propulsion Conf.*, 2010, pp. 1–6.

[139] L. Chen, H. Wang, B. Liu, Y. Wang, Y. Ding, and H. Pan, "Battery state-of-health estimation based on a metabolic extreme learning machine combining degradation state model and error compensation," *Energy*, vol. 215, Jan. 2021, Art. no. 119078.

[140] L. Cai, J. Meng, D.-I. Stroe, G. Luo, and R. Teodorescu, "An evolutionary framework for lithium-ion battery state of health estimation," *J. Power Sources*, vol. 412, pp. 615–622, Feb. 2019.

[141] Y. Li, H. Sheng, Y. Cheng, D.-I. Stroe, and R. Teodorescu, "State-of-health estimation of lithium-ion batteries based on semi-supervised transfer component analysis," *Appl. Energy*, vol. 277, Nov. 2020, Art. no. 115504.

[142] N. Noura, L. Boulon, and S. Jemeï, "A review of battery state of health estimation methods: Hybrid electric vehicle challenges," *World Elect. Veh. J.*, vol. 11, no. 4, pp. 66–85, 2020.

[143] L. R. Chen, "Design of duty-varied voltage pulse charger for improving Li-Ion battery-charging response," *IEEE Trans. Ind. Electron.*, vol. 56, no. 2, pp. 480–487, Feb. 2009.

[144] B. Tar and A. Fayed, "An overview of the fundamentals of battery chargers," in *Proc. IEEE 59th Int. Midwest Symp. Circuits Syst. (MWSCAS)*, Abu Dhabi, UAE, 2016, pp. 1–4.

[145] I. N. Moghaddam, B. Chowdhury, and M. Doostan, "Optimal sizing and operation of battery energy storage systems connected to wind farms participating in electricity markets," *IEEE Trans. Sustain. Energy*, vol. 10, no. 3, pp. 1184–1193, Jul. 2019.

[146] N. Nazir and M. Almassalkhi, "Guaranteeing a physically realizable battery dispatch without charge-discharge complementarity constraints," *IEEE Trans. Smart Grid*, early access, Sep. 2, 2021, doi: 10.1109/TSG.2021.3109805.

[147] F. Chang, Z. Zheng, and Y. Li, "PWM strategy of a novel cascaded multi-level converter for battery management," in *Proc. 17th Int. Conf. Elect. Mach. Syst. (ICEMS)*, Hangzhou, China, 2014, pp. 3208–3212.

[148] W. Choi *et al.*, "Reviews on grid-connected inverter, utility-scaled battery energy storage system, and vehicle-to-grid application-challenges and opportunities," in *Proc. IEEE Transp. Electrif. Conf. Expo (ITEC)*, Chicago, IL, USA, 2017, pp. 203–210.

[149] S. D. G. Jayasinghe, D. M. Vilathgamuwa, and U. K. Madawala, "A battery energy storage interface for wind power systems with the use of grid side inverter," in *Proc. IEEE Energy Convers. Congr. Expo.*, 2010, pp. 3786–3791.

[150] S. Burusteta, J. Pou, S. C. Recio, I. Marino, J. A. Anzola, and V. G. Agelidis, "Capacitor voltage balancing in a three-level-converter-based energy storage system," *Eur. Power Electron. Drives J.*, vol. 23, no. 4, pp. 14–22, 2013.

[151] L. M. Grzesiak and J. G. Tomasik, "Autonomous power generating system with multi-level converters," in *Proc. IEEE 32nd Annu. Conf. Ind. Electron.*, 2006, pp. 2815–2820.

[152] J. Chen, Y. Zhong, C. Wang, and Y. Fu, "Four-level hybrid neutral point clamped converters," *IEEE J. Emerg. Sel. Topics Power Electron.*, vol. 9, no. 4, pp. 4786–4801, Aug. 2021, doi: 10.1109/JESTPE.2021.3060906.

[153] L. S. Xavier, W. C. S. Amorim, A. F. Cupertino, V. F. Mendes, W. C. D. Boaventura, and H. A. Pereira, "Power converters for battery energy storage systems connected to medium voltage systems: A comprehensive review," *BMC Energy*, vol. 1, p. 7, 2019. [Online]. Available: https://doi.org/10.1186/s42500-019-0006-5

[154] S. Benner. "A brief history of regulation signals at PJM." [Online]. Available: https://www.pjm.com/-/media/committees-groups/committees/oc/20150701-rpi/20150701-item-02-history-of-regulation-d.ashx (Accessed: Jun. 9, 2015).

[155] X. Wu, J. Zhao, and A. J. Conejo, "Optimal battery sizing for frequency regulation and energy arbitrage," *IEEE Trans. Power Del.*, vol. 37, no. 3, pp. 2016–2023, Jun. 2022, doi: 10.1109/TPWRD.2021.3102420.

[156] H. Zhao, M. Hong, W. Lin, and K. A. Loparo, "Voltage and frequency regulation of microgrid with battery energy storage systems," *IEEE Trans. Smart Grid*, vol. 10, no. 1, pp. 414–424, Jan. 2019.

[157] D. Zhu and Y. A. Zhang, "Optimal coordinated control of multiple battery energy storage systems for primary frequency regulation," *IEEE Trans. Power Syst.*, vol. 34, no. 1, pp. 555–565, Jan. 2019.

[158] J. Tan and Y. Zhang, "Coordinated control strategy of a battery energy storage system to support a wind power plant providing multi-timescale frequency ancillary services," *IEEE Trans. Sustain. Energy*, vol. 8, no. 3, pp. 1140–1153, Jul. 2017.

[159] B. M. Gundogdu, S. Nejad, D. T. Gladwin, M. P. Foster, and D. A. Stone, "A battery energy management strategy for U.K. enhanced frequency response and triad avoidance," *IEEE Trans. Ind. Electron.*, vol. 65, no. 12, pp. 9509–9517, Dec. 2018.

[160] T. Zhao, A. Parisio, and J. V. Milanović, "Distributed control of battery energy storage systems for improved frequency regulation," *IEEE Trans. Power Syst.*, vol. 35, no. 5, pp. 3729–3738, Sep. 2020.

[161] M. Zeraati, M. E. H. Golshan, and J. M. Guerrero, "Distributed control of battery energy storage systems for voltage regulation in distribution networks with high PV penetration," *IEEE Trans. Smart Grid*, vol. 9, no. 4, pp. 3582–3593, Jul. 2018.

[162] J. Matevosyan. "Survey of grid-forming inverter applications." Jun. 2021. [Online]. Available: https://www.esig.energy/event/g-pst-esig-webinar-series-survey-of-grid-forming-inverter-applications

[163] S. D. Rao *et al.*, "Grid-forming inverters-real-life implementation experience and lessons learned," in *Proc. 9th Renew. Power Gener. Conf. (RPG Dublin Online)*, 2021, pp. 7–12.

[164] "Grid forming energy storage: Provides virtual inertia, interconnects renewables and unlocks revenue." 2020. [Online]. Available: https://go.hitachi-powergrids.com/grid-forming-webinar-2020

[165] M. Kintner-Meyer, "Regulatory policy and markets for energy storage in North America," *Proc. IEEE*, vol. 102, no. 7, pp. 1065–1072, Jul. 2014.

[166] *Electric Storage Participation in Markets Operated by Regional Transmission Organizations and Independent System Operators*, Fed. Energy Regul. Commission, Washington, DC, USA, 2018.

[167] I. Usera, P. Rodilla, S. Burger, I. Herrero, and C. Batlle, "The regulatory debate about energy storage systems: State of the art and open issues," *IEEE Power Energy Mag.*, vol. 15, no. 5, pp. 42–50, Sep./Oct. 2017.

[168] E. Nasrolahpour, J. Kazempour, H. Zareipour, and W. D. Rosehart, "A bilevel model for participation of a storage system in energy and reserve markets," *IEEE Trans. Sustan. Energy*, vol. 9, no. 2, pp. 582–598, Apr. 2018.

[169] (PJM, Norristown, PA, USA). *Q&A for Electric Storage Resource Participation Model*. (Feb. 2018). https://www.pjm.com/-/media/committees-groups/committees/mic/20180914-special/20180914-item-06b-faq-for-order-841.ashx

[170] (PJM, Norristown, PA, USA). *Order 841: Status quo in PJM*. (May 2018). [Online]. Available: https://www.pjm.com/-/media/committees-groups/committees/mic/20180510-special-electric/20180510-item-03a-esr-841-status-quo review.ashx

[171] (PJM, Norristown, PA, USA). *Current Rules for Electric Storage Resources, PJM Manual*. (May 2018). [Online]. Available: https://www.pjm.com/-/media/committees-groups/committees/mic/20180510-specialelectric/20180510-item-03b-all-manual-citing-of-esr-status-quo.ashx

[172] J. S. John. (Greentech Media, Boston, MA, USA). *New York Is Breaking New Ground in Allowing Batteries to Play in Multiple Markets*. (Sep. 2020). [Online].Available: https://www.greentechmedia.com/squared/dispatches-from-the-grid-edge/new-yorks-new-rules-for-opening-markets-to-energy-storage

[173] Y. Fen. (China Energy Storage Aliance, Bejing, China). *How Have Different Countries Facilitated the Participation of Distributed Energy Storage in Power Markets?* (Apr. 2020). [Online]. Available: http://en.cnesa.org/latest-news/2020/4/30/how-have-different-countries-facilitated-the-participation-of-distributed-energy-storage-in-power-markets

[174] C. Lackner, T. Nguven, R. H. Byrne, and F. Wiegandt, "Energy storage participation in the German secondary regulation market," in *Proc. IEEE/PES Transm. Distrib. Conf. Exposit. (T&D)*, 2018, pp. 1–9.

[175] K. Sharma and D. V. Shah, *Supercharged: Challenges and Opportunities in Global Battery Storage Markets*, Deloitte Center Energy Solutions, New York, NY, USA, May 2018.

[176] G. Kamiya. (Int. Energy Agency, Paris, France). *Energy Storage, More Efforts Needed*. (Nov. 2021). [Online]. Available: https://www.iea.org/reports/energy-storage

[177] (Sandia Nat. Lab., Albuquerque, NM, USA). *DOE Global Energy Storage Database*. 2016. [Online]. Available: https://www.sandia.gov/ess-ssl/

[178] B. Voran. "Burns & McDonnell Completes Construction at Largest Battery Storage Facility in the World." [Online]. Available: https://www.burnsmcd.com/insightsnews/in-the news/2021/08/largest-battery-storage-facility-in-world (Aug. 19, 2021).

[179] X. Xie, Y. Guo, B. Wang, Y. Dong, L. Mou, and F. Xue, "Improving AGC performance of coal-fueled thermal generators using multi-MW scale BESS: A practical application," *IEEE Trans. Smart Grid*, vol. 9, no. 3, pp. 1769–1777, May 2018.

[180] Y. Ohki, "News from Japan," *IEEE Electr. Insul. Mag.*, vol. 32, no. 2, pp. 64–66, May 2016.

[181] K. Uehara and H. Ikeda, "Recent and future situation of Japan's T&D system," *J. Int. Council Elect. Eng.*, vol. 6, no. 1, pp. 231–234, 2016.

[182] (Chugoku Elect. Power Col Inc., Hiroshima, Japan). *Demonstration Project utilizing Hybrid Storage Battery System in the Oki-Islands*. (2016). [Online]. Available: https://www.nedo.go.jp/content/100788813.pdf

[183] J. Engel, "Europe's largest energy storage project successfully connects to the grid," *Renew. Energy World*, to be published. [Online]. Available: https://www.renewableenergyworld.com/storage/grid-scale/

[184] Carmen. "Dalian-UET/rongke power—Battery energy storage system, China." Sep. 2021. [Online]. Available: https://www.power-technology.com/marketdata

[185] C. Doetsch and A. Pohlig, "Chapter: 13—The use of flow batteries in storing electricity for national grids," in *Future Energy*, 3rd ed., T. M. Letcher, Ed., Elsevier, 2020, pp. 263–277. [Online]. Available: https://doi.org/10.1016/B978-0-08-102886-5.00013-X

[186] *Q2 2020 executive summary, U.S. Energy Storage Monitor, Wood Mackenzie Power & Renewables*, U.S. Energy Storage Assoc., New York, NY, USA, Jun. 2020.

[187] S. Yao, P. Wang, and T. Zhao, "Transportable energy storage for more resilient distribution systems with multiple microgrids," *IEEE Trans. Smart Grid*, vol. 10, no. 3, pp. 3331–3341, May 2019.

[188] G. Hering. "Burning concern: Energy storage industry battles battery fires." [Online]. Available: https://www.spglobal.com/marketintelligence/en/news-insights/latest-news-headlines/burning-concern-energy-storage-industry-battles-battery-fires-51900636 (Accessed: May 24, 2019.)

[189] "Accident analysis of the Beijing lithium battery explosion." [Online]. Available: https://www.ctif.org/news/accident-analysis-beijing-lithium-battery-explosion-which-killed-two-firefighters (Accessed: May 25, 2021.)

[190] W. Li, *Risk Assessment of Power Systems: Methods and Applications*. Piscataway, NJ, USA: IEEE Press, 2014.

[191] D. Guo, L. Sun, X. Zhang, P. Xiao, Y. Liu, and F. Tao, "The causes of fire and explosion of lithium ion battery for energy storage," in *Proc. 2nd IEEE Conf. Energy Internet Energy Syst. Integr. (EI2)*, 2018, pp. 1–5.

[192] T. Zhou, C. Wu, B. Chen, H. Zhu, and Y. Liu, "Fire suppression and cooling effect of perfluorohexanone on thermal runaway of lithium-ion batteries with large capacity," in *Proc. IEEE 5th Conf. Energy Internet Energy Syst. Integr. (EI2)*, 2021, pp. 3783–3788.

[193] J. Li, Q. Wang, Y. Li, Y. Wu, and Y. Cui, "Research progress on fire protection technology of containerized Li-ion battery energy storage system," in *Proc. IEEE Sustain. Power Energy Conf. (iSPEC)*, 2021, pp. 1105–1109.

[194] A. Tripathy, A. Bhuyan, R. Padhy, and L. Corazza, "Technological, organizational, and environmental factors affecting the adoption of electric vehicle battery recycling," *IEEE Trans. Eng. Manag.*, early access, Apr. 21, 2022, doi: 10.1109/TEM.2022.3164288.

[195] U.S. Department of Energy (DOE). "Electric drive vehicle battery recycling and 2nd life apps." [Online]. Available: https://www.energy.gov/bil/electric-drive-vehicle-battery-recycling-and-2nd-life-apps (Accessed: May 2, 2022).

[196] Y. Zhang, Z. Zhou, Y. Kang, C. Zhang, and B. Duan, "A quick screening approach based on fuzzy c-means algorithm for the second usage of retired lithium-ion batteries," *IEEE Trans. Transp. Electrif.*, vol. 7, no. 2, pp. 474–484, Jun. 2021.

[197] Y. C. Fong, D. H. Wang, J. Mei, S. R. Raman, and K. W. E. Cheng, "Study and development of mixed repurposing EV battery system for stationary energy storage applications," in *Proc. 8th Int. Conf. Power Electron. Syst. Appl. (PESA)*, 2020, pp. 1–6.